Deliverable 4.2

Predicting the physical impact by towed demersal gears from fishing gear characteristics

Main Contributors:
Ana Ivanović, Moosa Esmaeili, Clara Casanovas
University of Aberdeen
(UNIABDN, UK)

Barry O'Neill, Keith Summerbell
Marine Scotland Science
(Mar Lab, UK)

SUMMARY

When towed demersal fishing gears interact with the seabed and the water column along which they are towed. The immediate impact these elements make is physical and studies have shown that these physical effects

(i)   can have broader ecological, environmental and biological implications and also

(ii)   can affect the economic performance of the fishing operation.

It has been shown that towed demersal fishing gears influence habitats, cause benthic mortality, release nutrients and re-suspend phytoplankton cysts and copepod eggs. In addition, the studies of the fuel efficiency of fishing trawlers have demonstrated that the combined contact and hydrodynamic drag of a demersal towed gear can account for up to 80% of the fuel consumed.

It is therefore important to develop predictive methodologies to assess and quantify the ecological and environmental impact of towed fishing gears. In order to be in a position to evaluate their economic performance we must first be able to predict their physical impact. This report informs of a study that combines numerical simulations, sea trials and laboratory experiments. Here we further develop the numerical modelling approach of Ivanović et al. (2011) established in the previous EU project, DEGREE which is able to calculate the penetration into the seabed, the sediment displaced and the associated drag and contact forces that occur when a fishing gear is towed across the seabed. We also report on the laboratory study that has examined the scaled models of gear components as well as seatrials.

The resulting predictions correspond very well with data from experimental trials at sea and underline the potential of using deterministic methodologies to assess and quantify the impacts of towed gears. To develop these types of methodologies the physical impacts need to be related directly to the resulting geochemical, biological and environmental effects such as nutrient enhancement and benthic mortality. The development of these models would enable a tool to direct fishing effort, identify and establish closed areas and develop environmentally friendly fishing techniques.

1 INTRODUCTION

Quantitative measurement of the response of benthic habitats to impact from towed fishing gears is of significant importance to the ecosystem and the long-term management of sustainable fisheries. Current literature indicates that the effects of trawling on the benthos have focussed on before/after, control/impact comparative studies. This research area has been proved important in terms of describing general trends and has, in general identified taxa that suffer high levels of mortality, and habitat types where impact is greatest. However, a limiting factor in this approach is the lack of prediction-based methodology which resulted in the development of a more mechanistic approach that allows trawling impact on the benthos to be estimated for a wider range of species and habitats. The main emphasis of this report is on numerical approach which is validated and supported by seatrials and experimental studies.

A finite element (FE) model of the interaction of on bottom fishing gear components and the seabed is developed using different soil models and features available within the Abaqus finite element software package. The resulting models are able to predict the penetration depth and drag force along with the sediment displacement associated with each gear component and the predictions are compared with the results obtained during sea trials.

This report therefore focuses on modelling the physical interaction between gear components and the seabed. In particular the penetration and disturbance to the seabed caused by (i) the roller clump of a twin trawl and (ii) a trawl door (iii) rock hoppers, are examined.

2 BACKGROUND

The impact that demersal or bottom trawling can have on benthic habitats and communities have been examined as part of a number of studies by Clark and Frid, 2001; Kaiser et al 2002; and Løkkeborg, 2005 identifying the influence they have on the seabed. There are also concerns that the release of nutrients and phytoplankton cysts from sediments in the wake of a towed gear may have significant effects on the water column (Dounas et al (2007)). The demersal trawl is one of the most common types of towed fishing gears. It consists of several components of which (a) the otter door, (b) the ground gear, (c) the bridles/sweeps, and for twin trawls, (d) the roller clump are in direct contact with the seabed (see Figure 1). To fully appreciate the ecological and environmental impact of towed demersal fishing gears, understanding the physical mechanisms involved is of significant importance. With such an understanding the assessment of the impact of different towed fishing gears can provide a means to develop gears with reduced impact.

Figure 1. Twin trawling assembly

Majority of the studies of the physical processes (related to towed fishing gears) have focussed on the hydrodynamic forces acting on the gears and the related netting/gear deformation (Le Dret et al., 2004, Priour, 1999, Bessonneau and Marichal, 1998, O'Neill, 1997,1999, O'Neill and Neilson, 2008). These studies have been used to develop numerical trawl models for scientific and engineering design purposes, however, none has modelled the detailed interaction of the seabed and the gear components that are in contact with it. Prat et al. (2008) produced a model to predict the contact forces between the seabed and the otterboard but with no modelling of the penetration into the sediment. Paschen et al. (2000), reported on the outcome of laboratory studies to examine morphological changes in the upper seabed layers due to beam trawls. A number of tests were carried out on a test bed to investigate the impact of dragged trawl elements on the upper sediment layers. The results, measured by laser, show that with higher contact pressures there is an increase in the penetration depths of the tracks of beam trawls within a range of 10–80mm depending on the gear weight, the towing speed and the type of strata. The impact of trawl door scouring on infaunal bivalves has been examined by Gilkinson et al, (1998). The interaction, reported in their work between the otter trawl door with the seabed was examined in a laboratory test tank using a full-scale trawl door model. It is reported that a furrow of 2cm was created during the tests and that two out of forty two specimens that were placed in the scouring zone showed major damage.

A number of recent studies examined the drag force associated with the elements being towed along the seabed. The time evolution of the stresses in the bed were analysed where large force fluctuations acting on the tool were obtained. The fluctuations of drag force have a decreasing exponential distribution but the mean force is well fitted with the results of a limit analysis with Coulomb's failure criterion. Palmer (1999) studied the speed effects occurring when blades and ploughs cut the saturated soil. In that work it has been pointed out that the ploughing forces increase greatly when the plough share forces dilatant soil to deform rapidly but that no such effect is noticed in dry soil. Zhao and Miedema (2001) derived a mathematical model of the cutting forces in saturated sand at large cutting angles. They applied the finite element method to predict the occurrence of boundary soil wedges in saturated soil and to evaluate the interaction between the sand dilation and the existence of a dead zone in front of the blade. Igland and Søreide (2008) used the ANSYS software package to investigate the contact between a roller clump and marine pipelines where the seabed was modelled as a rigid surface and the contact between the pipeline

and the seabed surface was described by the Coulomb friction model. Although this model can predict the contact loads between the components no estimation of seabed penetration can be obtained due to the rigid nature of the surface and so no studies related to the soil were performed. More recently, Ivanović et al (2011) developed finite element models of the interaction between the seabed and trawl doors and clump weights using a Lagrangian numerical formulation.

The work undertaken by Paschen (2002, 2005) is based on the physical scale modelling studies of the contact forces between the seabed and ropes and chains, examining the morphological changes in the upper seabed layers due to trawl fishing gear as part of EU project, TRAPESE.

A number of studies related to penetration into soil have been carried out in other fields. Nouguier et al (2000) examine soil cutting processes by modelling the soil as a dry granular material and report that the main disturbance of the soil lies along a line of soil passing through the bottom of the tool. Two- and three-dimensional simulations of wheels on soils are carried out in Hambleton and Drescher (2009a, 2009b) by examining the impact of rigid and rolling cylinders on an elastic-perfectly plastic cohesive material that obeys the von Mises yield condition. A range of aspect ratios (width/radius) are considered by increasing the cylinder width and the authors find: that three-dimensional considerations are important (especially for narrow wheels); that quantitatively similar behaviour was obtained regardless of whether the soil stiffness is homogeneous or varies along the path; and that multiple narrow wheels have less rolling resistance but greater penetration than a single wide wheel. A similar model to investigate the impact of a cylindrical clump weight and an otter trawl door on a cohesive soil was developed by Ivanovic et al (2011) who validated their approach by comparing the results from experimental sea trials with model predictions. Both studies use finite element Abaqus software package where Arbitrary Lagrangian-Eulerian (ALE) mixed formulation was used.

3   MODEL DESCRIPTIONS

This report brings together the results of several different studies that have examined the effect of bottom trawling on different types of sediments. It combines the results of empirical and modelling studies, and synthesizes the available knowledge from the literature in order to give the most comprehensive overview of the topic so far. As indicated before, there are three streams of this project where the main part is numerical modelling which is accompanied by laboratory studies and seatrials for the validation purposes.

NUMERICAL MODELLING

The simulations were performed using the finite element code ABAQUS 6.10 in the Explicit mode, which performs a full dynamic analysis, but readily regains a quasi-static solution when boundary conditions are smoothly applied and the process is simulated over sufficiently large time. The schematic of the model used for simulating the soil–disk interaction using coupled Eulerian and Lagrangian method (CEL) is described in Esmaeili and Ivanović (2014) and Esmaeili and Ivanović (2015). The bed of soil consists of two regions, i.e. initial seabed material and the absence of material (void). The void region is necessary because the material flows into the mesh within the Eulerian domain, therefore the space is needed to retain this deformed material. This region is initially empty, but once the contact between the object and bed is made this region will occupy both the Lagrangian elements or/and Eulerian material. A schematic representation of the domains is shown in Figure 2.
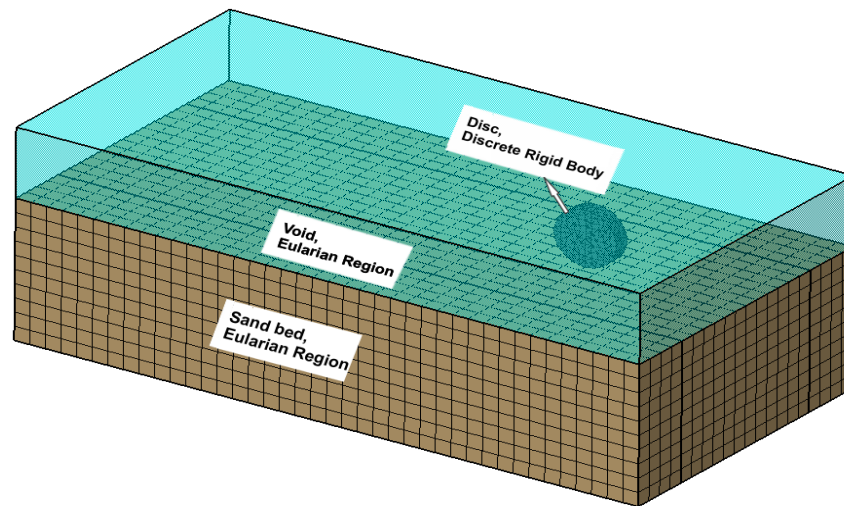
Figure 2 schematic representation of the FE model

In addition, since the radius and width of the clump were varied in this study, care was taken to ensure that the element size within the FE model was the same for each element design in order to avoid any potential discrepancy in results.

The soil was discretized using linear, 8-node, reduced integration, hexahedral brick elements. The clump was modelled as an analytical rigid surface and was governed by a single reference mode. The gravitational force on the shaft assembly is defined by applying a point force at a reference node located at the centre of mass of the clump. The seabed is generated as a rectangular block 2.4 m wide, 5.0 m long and 1.0 m deep and is assumed to be weightless. Fixed boundary conditions were applied to the bottom surface of the seabed while the long side faces were restrained in the lateral direction and the front and back faces were restrained in the longitudinal direction.

The numerical modelling of large deformation with the classical finite element method based on the Lagrangian formulation is extremely challenging. The Lagrangian approach has been used in a similar study but was proven sensitive to mesh distortion and is therefore deemed not sufficient enough to these problems. An Eulerian mesh however, can overcome the Lagrangian mesh distortion. The differences between Lagrangian and Eulerian meshes are most clearly seen in terms of the behaviour of the nodes. The description of this approach and the differences from the pure Lagrangian mesh approach is clearly described and elaborated on in Esmaeili and Ivanovic (2014).

Muddy sediment models

The elastic-perfectly plastic model, when used as a constitutive model for soil, assumes that the soil behaves in a linear elastic manner up to the yield stress after which it behaves plastically. It does not include strain hardening. It has been widely used in solving geomechanical problems for soils in undrained conditions and is appropriate for fully saturated soil. Despite being an approximation of the true soil response, it is often used as a reference for more advanced constitutive models. The failure criterion for soils is the von Mises criterion. This failure criterion is similar to the Tresca model. However, unlike the Tresca criterion, the von Mises criterion assumes that the intermediate principal stress also influences the material's response. It is defined by the shear yield stress $k=Y//\sqrt{3}$ where Y is the uniaxial yield stress elastic characteristics of the model reflect the condition where the Poisson's ratio is set to 0.49, the closest point to the saturated level. The soil from the experimental site was assumed to have had a density of 1900 kg/m^3 and laboratory tests on samples collected estimated a d_{10} = 13.9 µm, a Young's modulus of 2 MPa and a yield stress of 18 kPa, the values of which are used as a reference soil in this study.

Sandy sediment models

The sand is modelled as an Eulerian domain where the flow of the material in the mesh is tracked by computing its Eulerian Volume Fraction (EVF). The length of the sand bed is chosen long enough to ensure that the towing force has reached a steady state. Since the disk and roller were assumed to be non-deformable during the towing process it was modelled as a rigid body and discretised by using Lagrangian mesh, as represented in Figure 3. The weights are applied at a node located at the centre of the objects. To avoid large deformations at the beginning of the simulation, the object is allowed to penetrate in vertical direction without any movement in the horizontal direction. The geometry of the object is defined by two variables: diameter d and thickness t. The vertical penetration of the object, so-called sinkage is denoted as z. The vertical and horizontal component of the reaction force at the centre of the object are denoted as F_V and F_H, respectively.
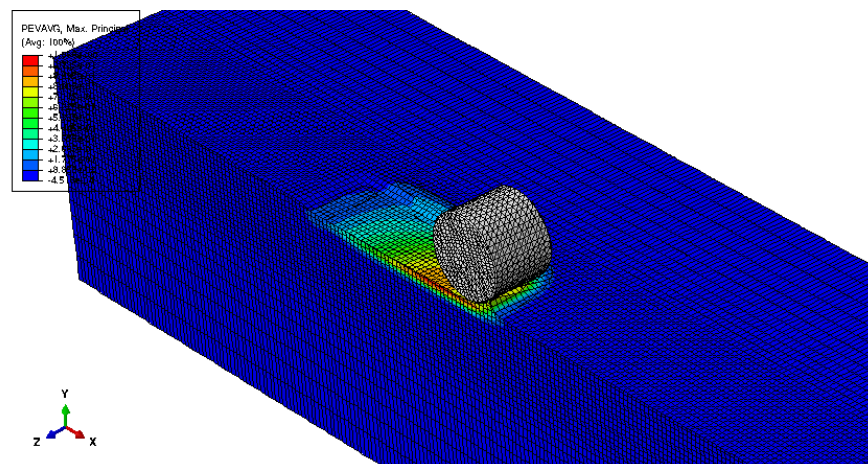
Figure 3 FE model of the roller clump

4   EXPERIMENTAL TRIALS

Experimental trials were carried out in the laboratory and at sea to collect data with which to validate and test the numerical models.

Laboratory trials

The experimental investigations were undertaken to evaluate experimentally the ground forces and the amount of disturbed sediment, focusing on the mount of soil formed in front of the ground fishing gear during bottom trawling when dragged along the seabed from the reduced scale modelling.

Materials and Methods

Experiments were conducted in a 4.8m long, 0.8m wide and 0.3m water depth channel with a mechanical frame consisting of two rails specially designed and constructed on top of the channel (Figure 4). A trolley to which a gear component can be attached is pulled mechanically through the rails by a system of wires. The trolley is equipped with a load cell which measures load in all three (longitudinal, transversal and vertical) directions and an LVDT that measures the displacement of the model in vertical direction i.e. penetration into the soil.
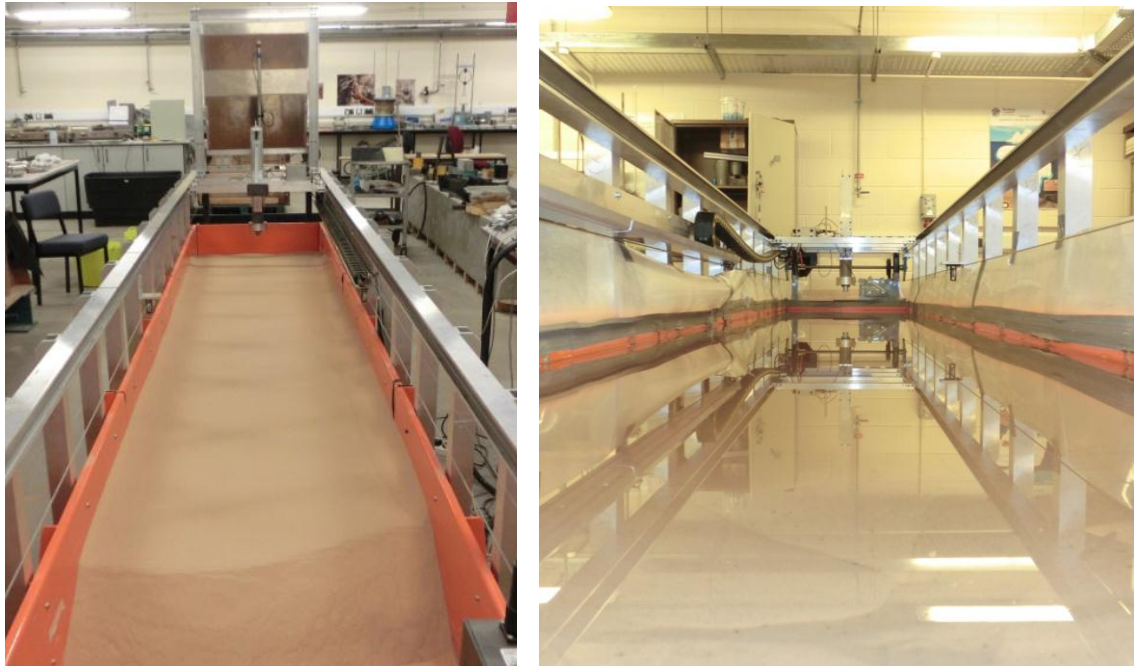
Figure 4 Sand channel facility at dried (left) and saturated conditions (right)

Reduced scale models (shown in Figure 5, Figure 6 and Figure 7) were attached to the load cell and dragged at dried and saturated conditions, at different predetermined fixed penetration depths along the sediment bed prepared in the channel. Forces from each experiment were obtained by averaging the force response obtained from the load cell (Figure 9) over 10 to 15 sec time period once steady state was reached. The same procedure was followed to obtain the water pressure signal gathered by the pressure transducers (Figure 10) placed on the interface cylinder-soil. Water pore pressure variations within the soil mass and in the interface between the model and the soil during dragging were measured by means of pressure transducers conveniently placed in the ground and at the interface as shown in Figure 8, an example of the signal gathered is shown in Figure 11.
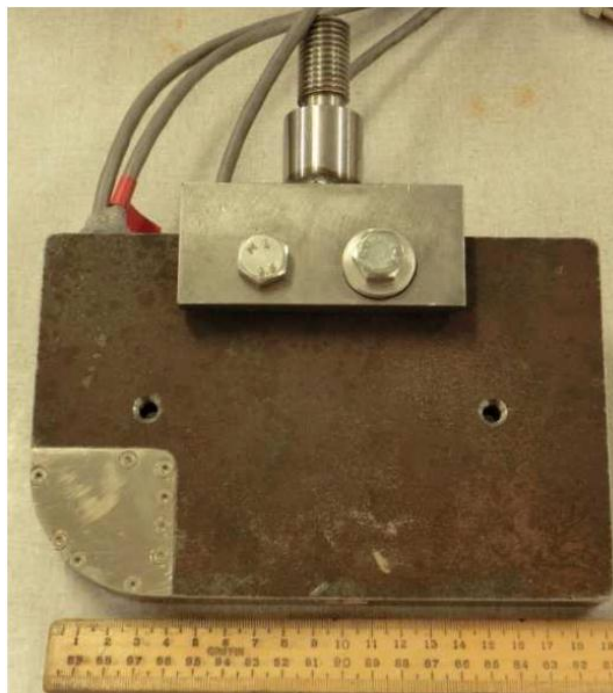
Figure 5 Gear element models reduced to 1:10 otter-door model (left) and 1:5 roller clump (right)
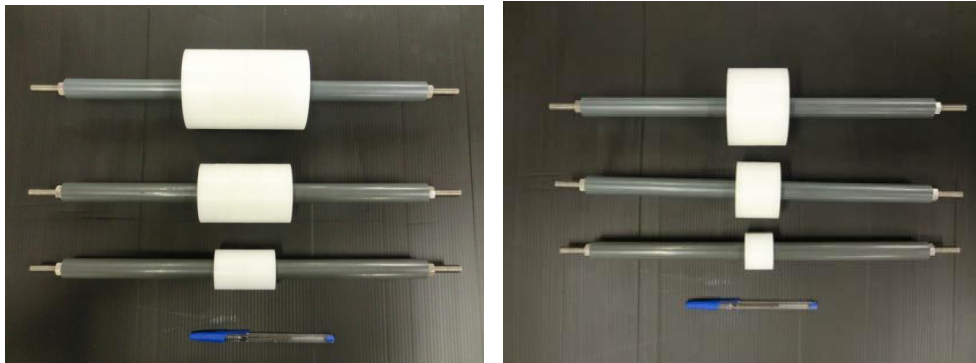
Figure 6 Wide (left) and narrow (right) group of geometrically similar reduced scale rock-hoppers
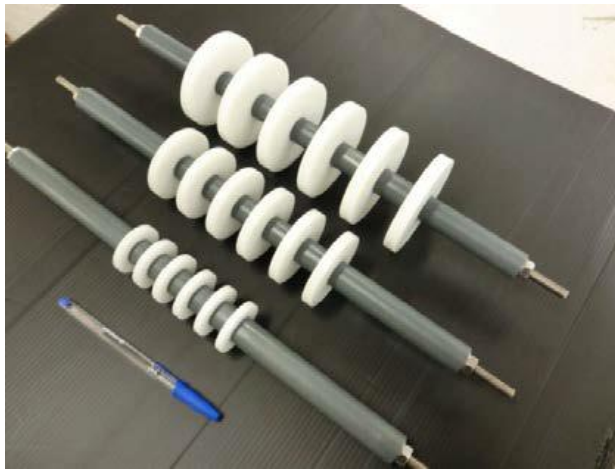
Figure 7 Group of geometrically similar reduced scale disks

The sediment used in the study was uniformly graded silica sand which was carefully prepared, where the sand surface was prepared at medium-dense state (50% relative density) by raking and flattened before any test run. Relevant sand properties obtained from standard soil testing are presented in Table 1.

D_{50}	0.177
C_u	1.43
Sand bed relative density	50 %
Average γ_{dry}	15.68kN/m^3
Average k	0.00033m/s
φ'	32°
$\delta_{steel-sand}$	22.3°

Table 1 Sand properties
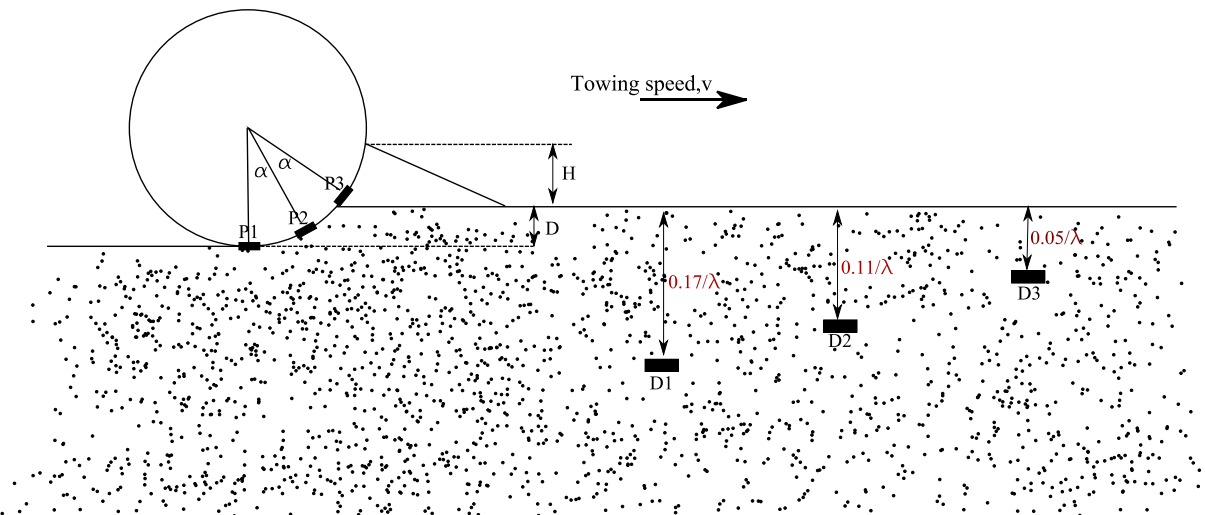
**Figure 8** Position of the water pore pressure transducers in the experimental set-up (α=25°) for the case of non-rolling cylindrical shape ground gear

Figure 11 shows relevant results for the suction measured within the soil immediately above the models as they approached and then passed over the transducers. As plotted in Figure 11, pore pressure transducers detected the approach of the model with a slight increase in the pore pressure, this is followed by a reduction in pore pressure as the model approaches the position of the transducer. Before undertaking experiments, the equipment employed to get experimental data was calibrated to ensure the reliability of the data collected.
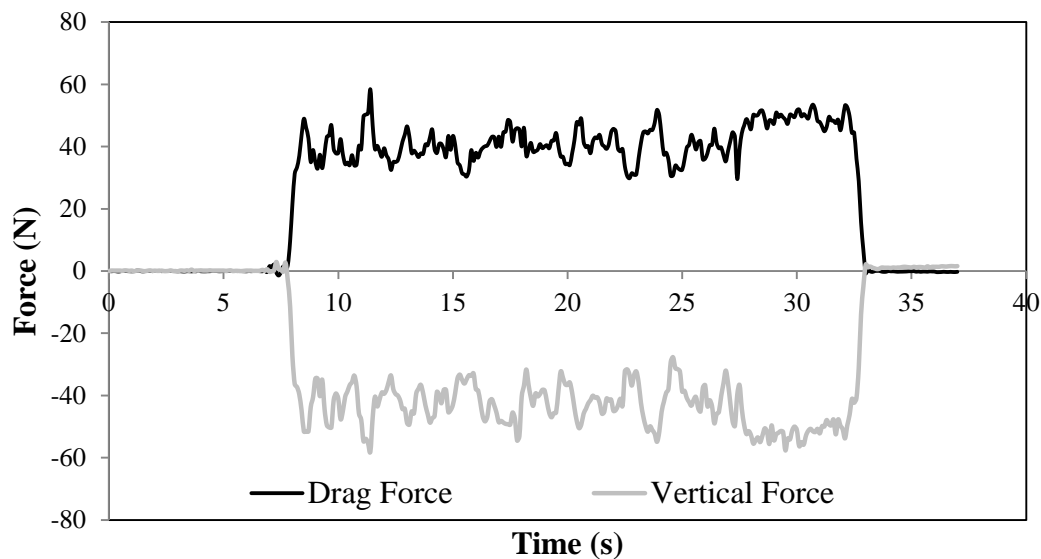
Figure 9. Forces signal registered for the 0.16m diameter cylinder (λ=1.5), dragged at 6mm depth and 0.07m/s.
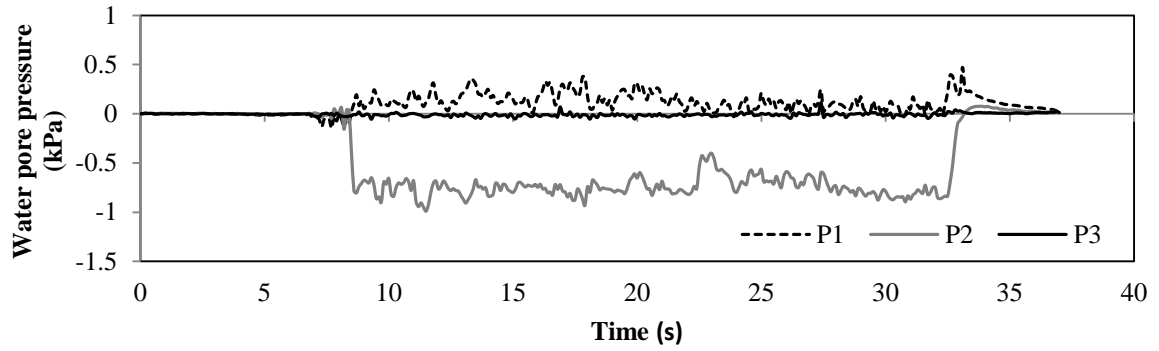
Figure 10. Water pore pressure measured at the interface of the 0.16m diameter cylinder (λ=1.5), dragged at 6mm depth and 0.07m/s.
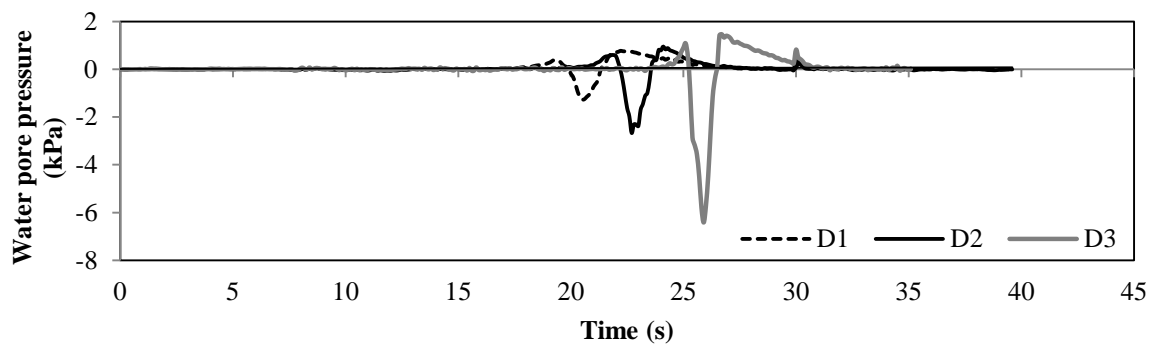
Figure 11. Water pore pressure measured within the soil mass at different depths for the 0.16m diameter cylinder (λ=1.5), dragged at 6mm depth and 0.07m/s.

Morphology of the frontal mound of sand developed immediately in front of the models during dragging and its evolution along the experiment is evaluated. See example in Table 2.

Speed	1:10 reduced scale Otter-door model
0.01m/s	

0.03m/s	
0.07m/s	
0.11m/s	
0.138m/s	

Table 2. Evolution of the frontal mount in front of a cylindrical towed element with the increase of the velocity for the otter-door at a penetration depth of 0.005m and 30° angle of attack

Scalability of the Forces

Three geometrically similar ground-gear models at different scales (λ=1, 1.5 and 2), with a value of aspect ratio (width:diameter) of 0.75, are specially designed to undertake this study. See more details in Figure 12 and Table 3. Dimensionless values for the depths (D=z/d) were set-up at 0.0625, 0.05 and 0.0375. Five different towing speeds (0.001, 0.03, 0.07, 0.11 and 0.138m/s) were tested at saturated conditions whereas a unique towing speed of 0.03m/s was tested at dried conditions. Forces evaluated from dried conditions correspond well to the fully drained situation (at a very slow towing speed or quasi-static).
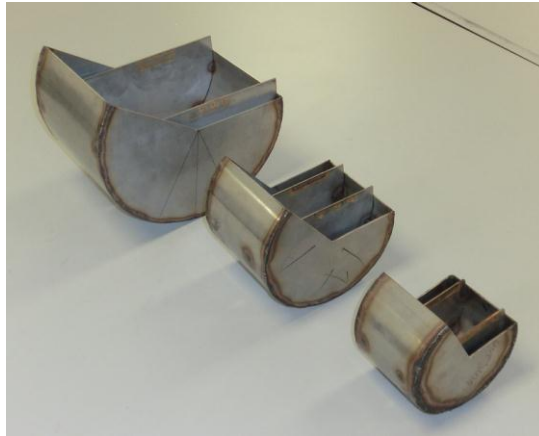
Figure12 Geometrically similar set of simplified cylindrical ground fishing gear

Scale 1:λ	Radius (m)	Width (m)
1:1	0.24	0.18
1:1.5	0.16	0.12
1:2	0.12	0.09

Table 3 Dimensions of the geometrically similar set of simplified fishing gear employed to evaluate scalability issues

Figure 143presents average results for the group of geometrically similar cylinders scaled up to full scale by the cube of the scale factor (λ). As shown, forces increase linearly with the increase of the towing velocity until values up to 0.12m/s, where depending on the case a decrease or different trends are found. For modelling different scaled models, towing velocity was kept the same for each reduced scale model and no effect related to this parameter was found in the scaled up version of the ground forces (drag and vertical). Very good agreement for both forces drag and vertical is observed for most of the penetration depths and towing velocities tested. However, some disagreement is noticed for the drag force at the faster towing velocity for the reduced scale models with the respect to the full scale element. A decrease of the drag force is found for the 1:2 reduced scale model drag force when the towing speed greater than 0.12m/s is achieved whereas for the 1:1.5 reduced scale model this force tends to remain constant.

On the other hand, a decrease in the vertical component of the ground reaction was found for all the elements. This decrease in the forces may be due to liquefaction phenomenon happening in the frontal area of the cylinders as observed in the last row of Table 4 where an important effect due to the towing speed is observed on the morphology of the frontal mount.
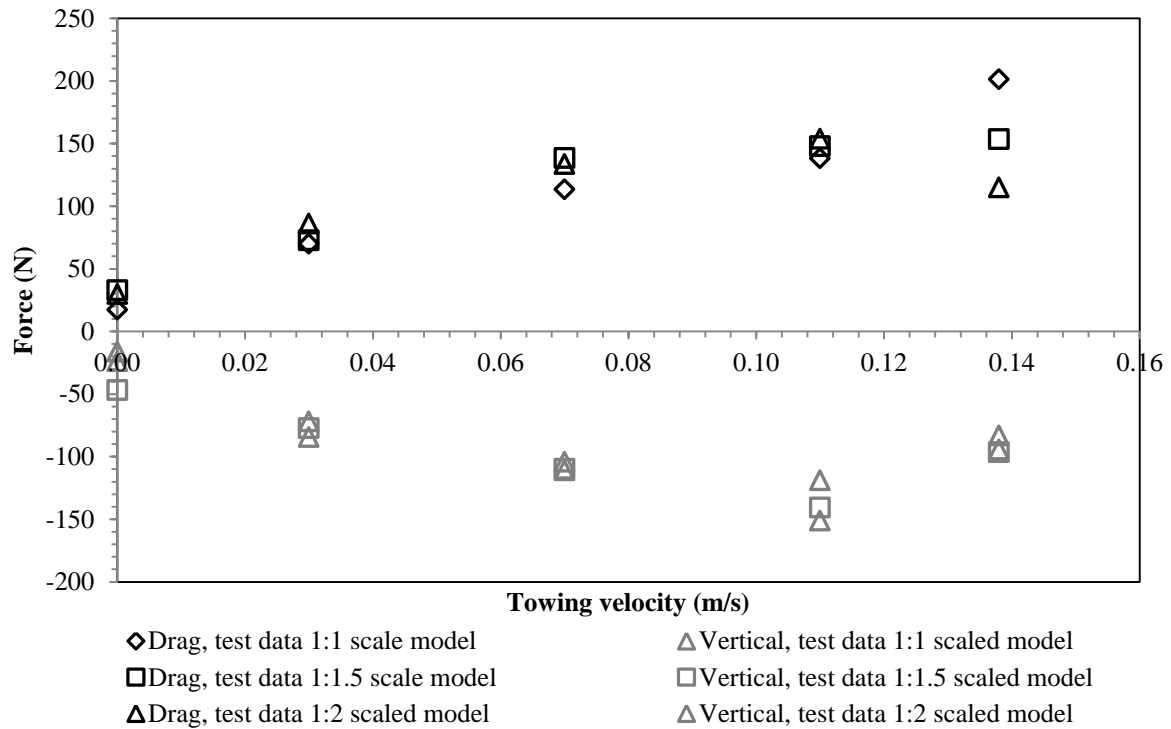
Figure 13. Variation of the drag and vertical forces for the geometrically similar cylinders with the increase of the towing velocity 1:1, 1:1.5 and 1:2 scales at a dimensionless penetration depth of 0.0375 (Results shown at a prototype scale)

However, a last point must be related to p_{amb} validated before we can confirm this hypothesis. Tests were carried out at $p_{amb} \approx p_{atm}$, but bottom trawling takes place at higher pressures. For example, if the trawling activity takes place at 30m depth, p_{amb} is approximately three times p_{atm}. Therefore, it could be of great importance that the scaling of the p_{amb} for all three cases is evaluated to confirm conclusions obtained from the experimental study and therefore the prediction of the forces due to the ground reaction.

**Scalability of the soil structures resulting from the ground fishing gear**

Scalability of the dimensions of the frontal mount (see each case studied for a given dimensionless penetration depth in Table 4) by the length scale factor (λ) was confirmed and therefore the capacity of modelling to predict the volume of soil disturbed and displaced during trawling by the ground gear is validated. Results are presented in Figure 14.
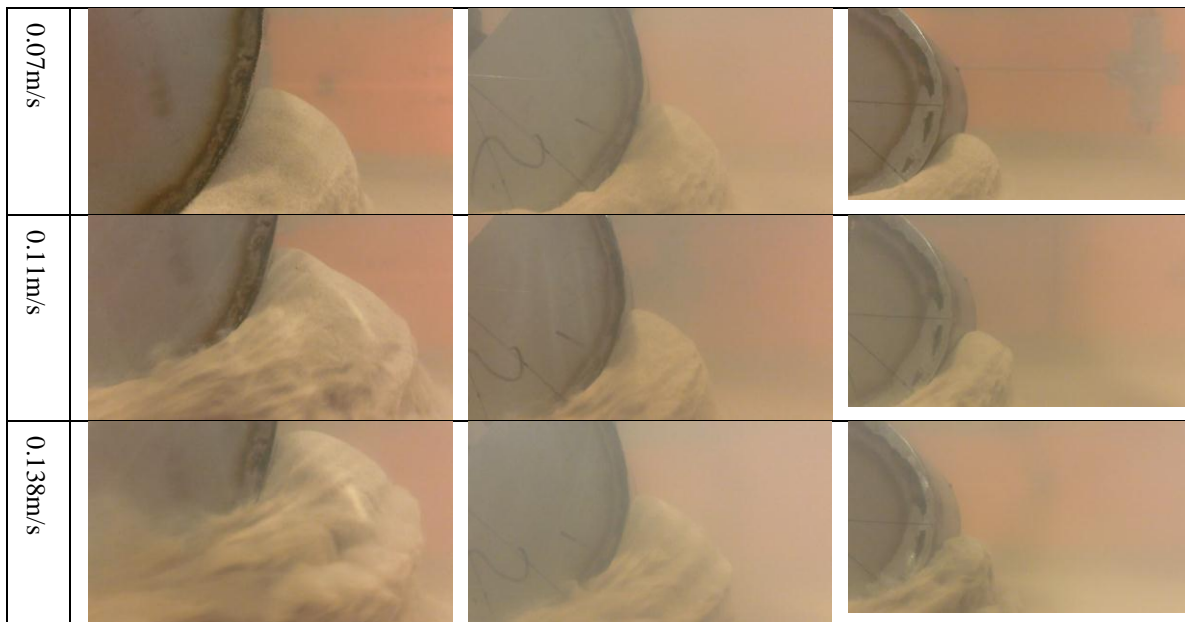
Table 4. Frontal mount of sand at steady state for each model and towing velocity for a dimensionless penetration depth of 0.05
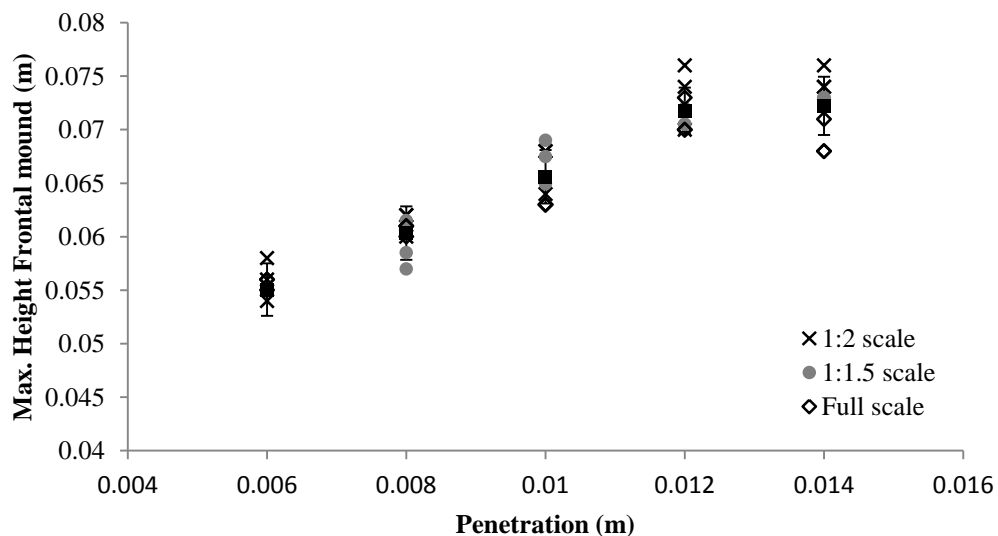
Figure 14 Evolution of the frontal mound for the simplified geometrically similar cylindrical fishing gear models towed along the sand at very shallow penetration depth

Reduced Scale Modelling

The present experimental work has been carried out by using sand similar to the sediment found in commonly bottom trawled areas in the North Sea (Netherlands, Belgium & Scotland) in terms of particle size distribution and strength properties. Due to the issue related to the required fixed penetration depth required to carry out the experiments, reported penetration depths were evaluated from field observation reported in literature (summarized in Table 5) to work out the range of reduced scale penetration depths relevant for the study with reduced scale models towed along the sandy sediment.

Caddy (1973) reported that an otter-door dragged along sandy sediment penetrates few centimetres on the ground, which agrees with the observation from Bridger (1970) who founds that the dragged otter-door affects a thin layer of top subtracted. On the other hand Jones (1992) evaluated muddy and sandy sediments and found that the penetration into the ground ranges from few mm to 300 mm, which is

deeper for muddy sediments. Arntz and Weber (1970) found that for muddy fine sand the penetration depth of the otter-door ranged between 100-150mm. Krost et al. (1990), evaluated penetration depth in sand and mud sediments finding the penetration depth ranging between 5-200mm. Khandriche et al. (1986) found otter-door penetration depths about 200mm in muddy sediment. Since the penetration in sand is smaller in sand than in mud, the value of 5mm penetration depth found by Krost et al. (1990) is therefore taken as the minimum value for the penetration of the otter-door to set-up the penetration depth. The maximum value considered in this study is related to the range of penetration depths found by Arntz and Weber (1970), being 100mm penetration depth the value considered. In conclusion, a range of penetration depths between 5 and 100mm will be scaled down and studied by the otter-door.

A few references were found in literature for the penetration of the ground-gear. Krost et al. (1990) reported on penetration depths between 20 and 50mm for muddy and sandy grounds, respectively however the size of the rollers was not specified. In the present study 20mm penetration depth is taken as the minimum value for the penetration depth but higher values than 50mm (until 150mm) are considered to evaluate the force trends as a function of the penetration depth.

Penetration Depth	Reference	Gear type	Sediment type
100-150 mm	Arntz and Weber, 1970	Otter-doors	Muddy fine sand
a thin layer of top substrate	Bridger, 1970	Otter-doors	Sand
few centimetres	Caddy, 1973	Otter-doors	Sand
200 mm	Khandriche, et al., 1986	Otter-door	Mud
5-200 mm	Krost et al, 1990	Otter-door	Mud, sand
20-50 mm		Rollers on foot rope	
5-170 mm	Rumohr (in Krost et al, 1990)	Otter-door	Mud, sand
few mm. - 300 mm	Jones, 1992	Otter-door	Mud, sand (deepest in soft mud)
~ 140 mm	Lindeboom and de Groot (edit.), 1998	Otter-door	Mud

Table 5. Summary of reported penetration depth for the otter-door and ground-gear (rollers) (extracted from Linnane et al. (2000))

Finally, a range of penetration depths considered for the roller clump is determined by considering findings reported in Ivanović et al. (2011) which are above or below the reported values included in the work for research purposes.

**Determination of the drag forces due to the interaction of the fishing rig with the seabed**

Otter-door

Ground forces due to the interaction of the otter-door with the seabed are evaluated in dried conditions as a function of the angle of attack and the penetration depth at a given speed. However, in saturated conditions velocity forces are also evaluated as a function of the towing velocity. Figure 15 shows the measured force components acting on the otter-door when dragged at v=0.03m/s at 5mm penetration depth in loose dry sand. Note that for angles between 25 and 35, magnitude of all three force components is similar. Figure 16, Figure 17 and Figure 18 show in more detail drag, vertical and lateral force components respectively. Despite the dispersion in results found for the lateral component, a linear increase of the forces with the angle of attack is found.

Figure 19 presents drag force component evaluated for the otter-door towed at 30° angle of attack at different penetration depths (from 5 to 30mm), showing that ground forces increase linearly with the increase of the penetration depth. No influence in terms of forces is found when the otter-door is dragged at different towing velocities at dried conditions.
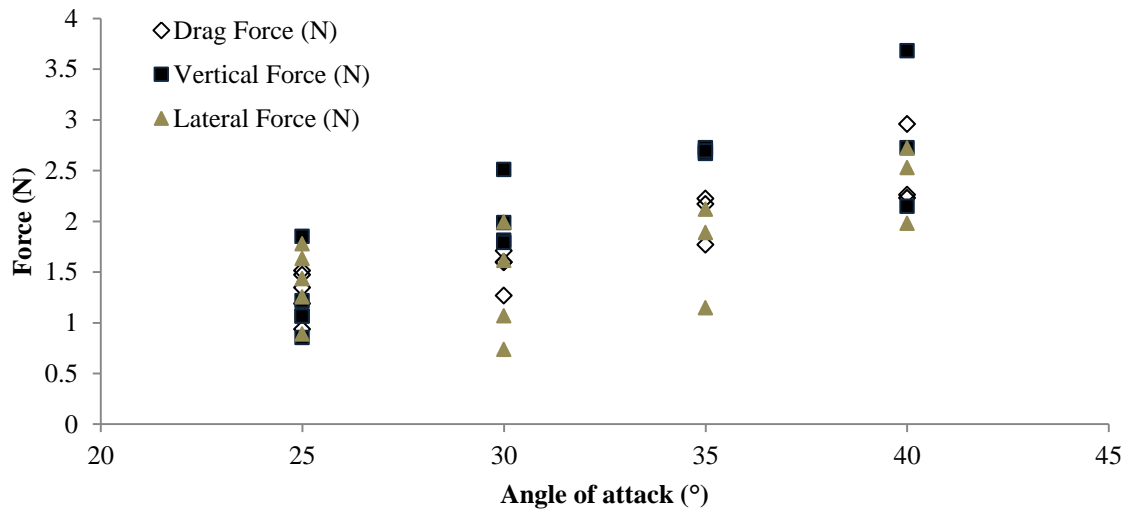

Figure 15 Comparison of the forces for the otter-door dragged at angles of attack comprised between 25 and 40° at 5mm penetration depth in loose dried sand
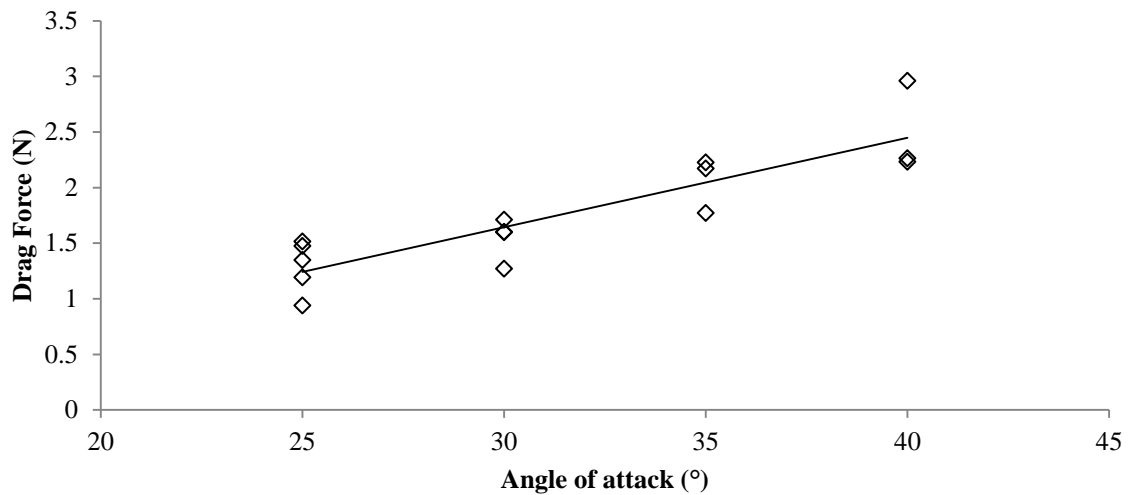

Figure 16 Drag forces for the otter-door dragged at angles of attack comprised between 25 and 40° at 5mm penetration depth in loose dried sand
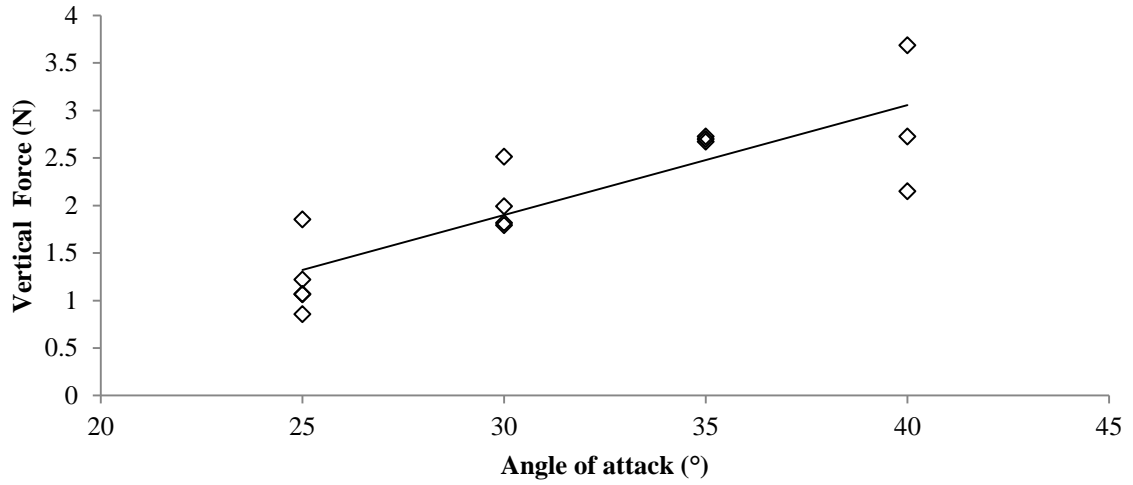
Figure 17 Vertical forces for the otter-door dragged at angles of attack comprised between 25 and 40° at 5mm penetration depth in loose dried sand
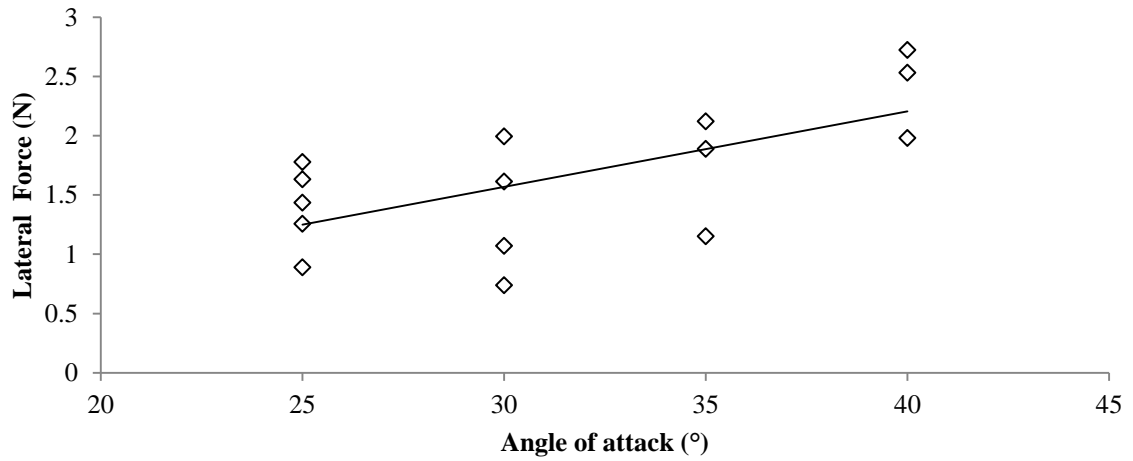

Figure 18. Lateral forces for the otter-door dragged at angles of attack comprised between 25 and 40° at 5mm penetration depth in loose dried sand
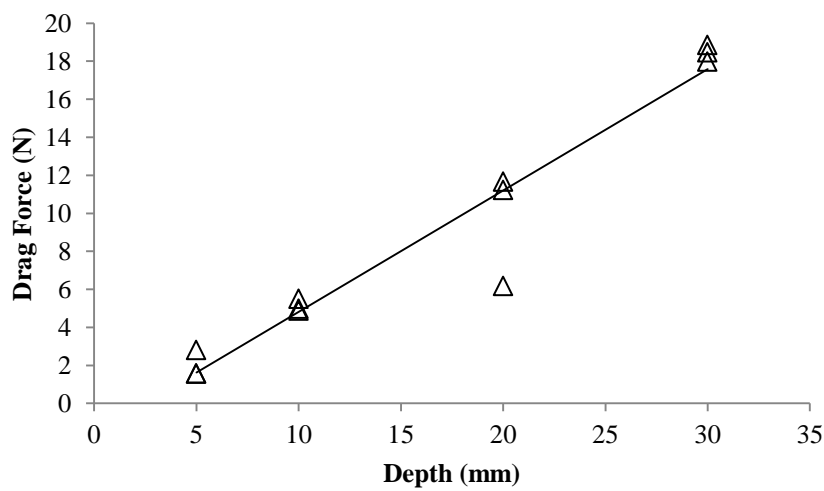
Figure 19. Drag forces for the otter-door dragged at 30° angle of attack at penetration depths comprised between 5 and 30mm in loose dried sand

However, when reduced scale otter-door model is towed along the sand bed at dried conditions a rate effect related to the towing velocity is found. Figure 20 shows mean values found for the drag force component when the otter-door model is dragged along the sand bed at 30° angle of attack and for a range of penetration depths between 3 and 5mm. Note that forces increase linearly with the increase of the velocity until a towing velocity of 0.1m/s, where due to liquefaction of the sediment (see Table 2) they tend to remain constant. Note that drag forces evaluated at towing velocity of 0.01≈0m/s are coincident to those evaluated at dried conditions since fully drainage is achieved.
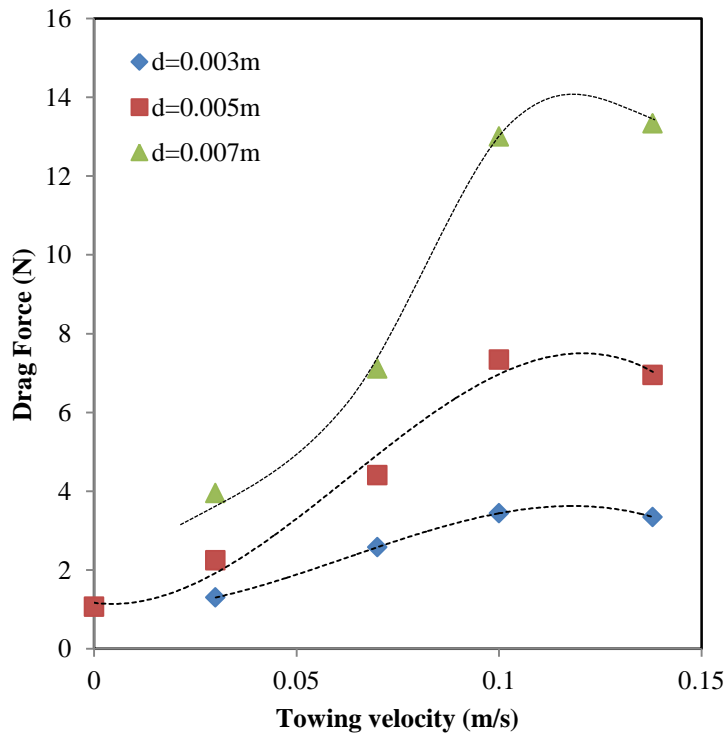

Figure 20 Drag force vs. Towing velocity for the 1:10 reduced scale otter-door model dragged in saturated conditions in loose sand at penetration depths of 3, 5 and 7mm.

Assembly of six Disks

Results for the scaled up to full scale drag and vertical ground forces evaluated from tests conducted by the set of arrangement of six disks models at different angles of attack are presented in Figure 21 and Figure 22. Experiments were undertaken in dried sand at loose conditions. The dimensionless separation (ratio between the separation of the discs and its diameter) between discs was 3.75. Models were dragged at constant towing velocity of 0.03m/s. Drag forces results plotted in Figure 21 suggest that the angle of attack for the assembly of disks has very small or no influence in the drag component of the ground reaction. However, the vertical component which magnitude is greater than the drag force component seems to decrease with the increase of the angle of attack as shown in Figure 22. Note that the negative sign of the vertical component indicate the upwards direction of the force. Also note the good scalability of the forces from all three scales evaluated.
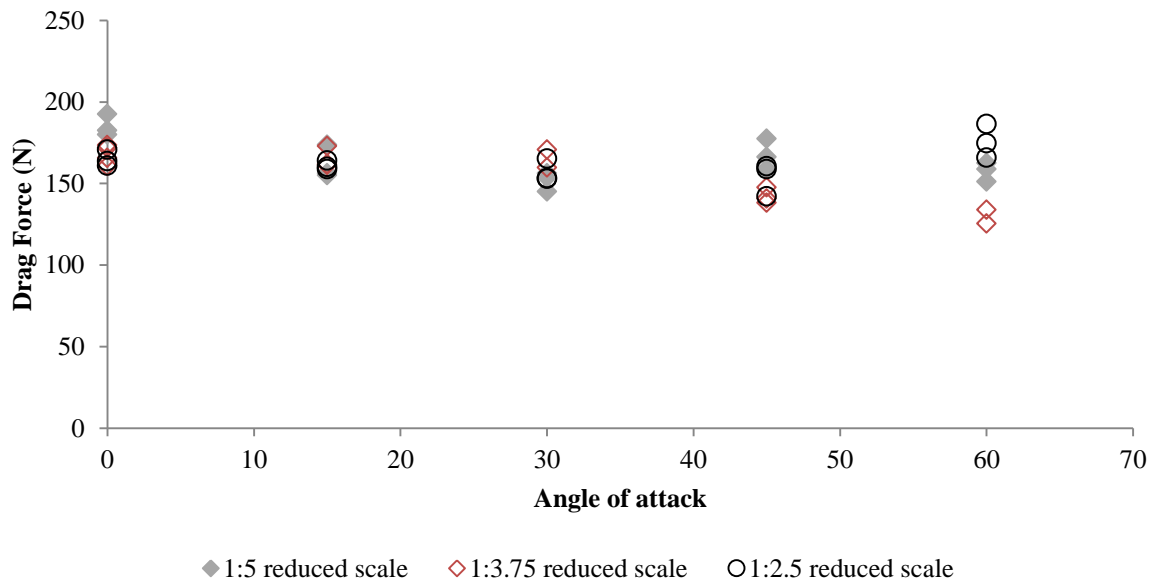
Figure 21 Scaled up to full scale drag force vs. angle of attack for the set of reduced scale disk assembly dragged in dried sand at a dimensionless penetration depth of 0. 0.1167
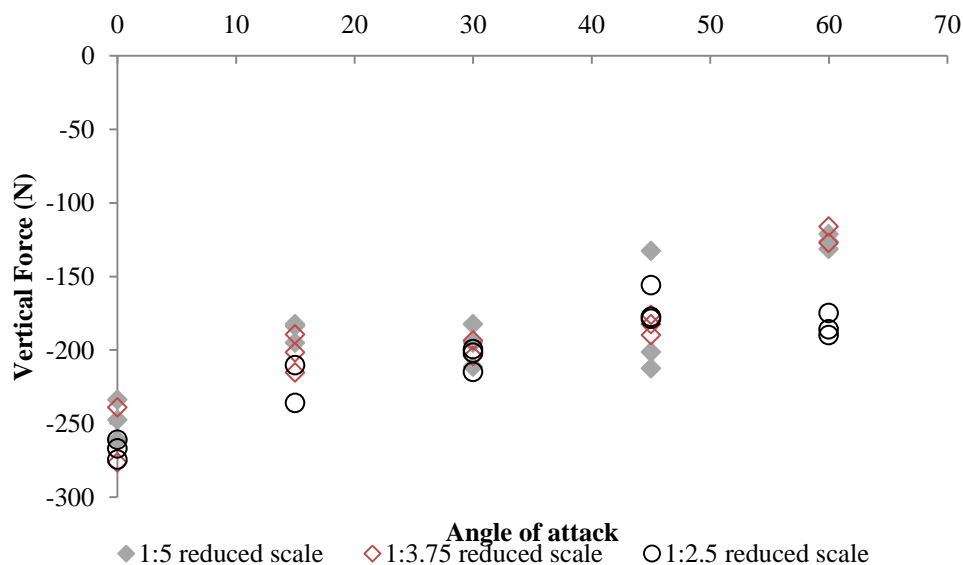

Figure 22. Scaled up to full scale vertical force vs. angle of attack for the set of reduced scale disk assembly dragged in dried sand at a dimensionless penetration depth of 0.1167

Another interesting point considered in the study of the assembly of disks is the influence of the separation of disks. For that, ground forces are evaluated by using the 1:2.5 reduced scale assembly of disks at 0° and at an only penetration of 14mm considering three different disk separations (45mm, 30mm and 22.5mm). Results are shown in Figure 23. The trend shows an increase of the forces with the decrease of the spacing between the disks in the arrangement. The increase of the soil reaction when the separation of the disks decreases could be due to the interaction of the individual failure zones beneath the individual disks (Figure 24) resulting an interaction comparable to an interacting wide cylinder (see Figure 25 and Figure26).
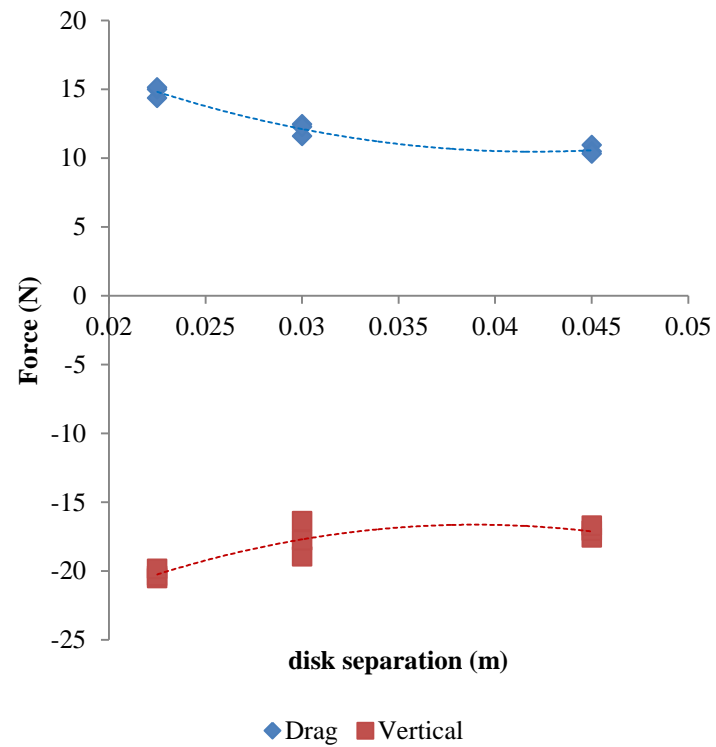
Figure 23. Drag and Vertical ground forces vs. separation of the disks in the experimental arrangement of 6 disks.
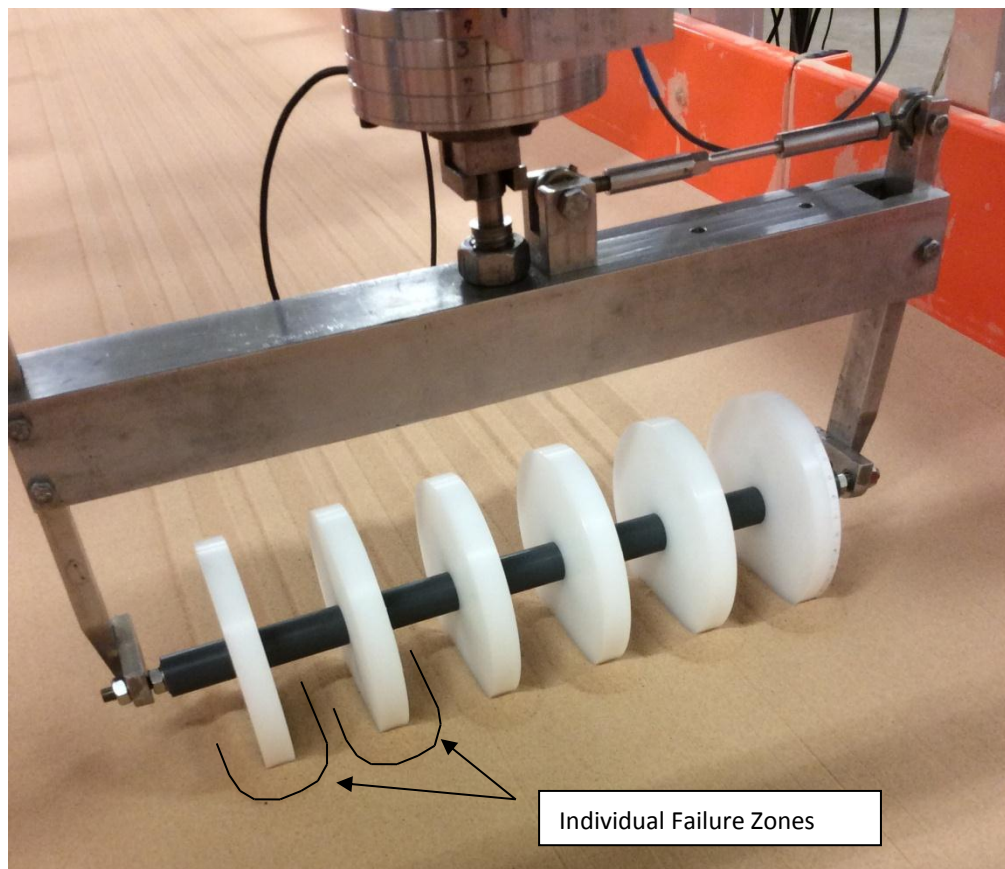
Figure 24 Disks arrangement with 45mm spacing
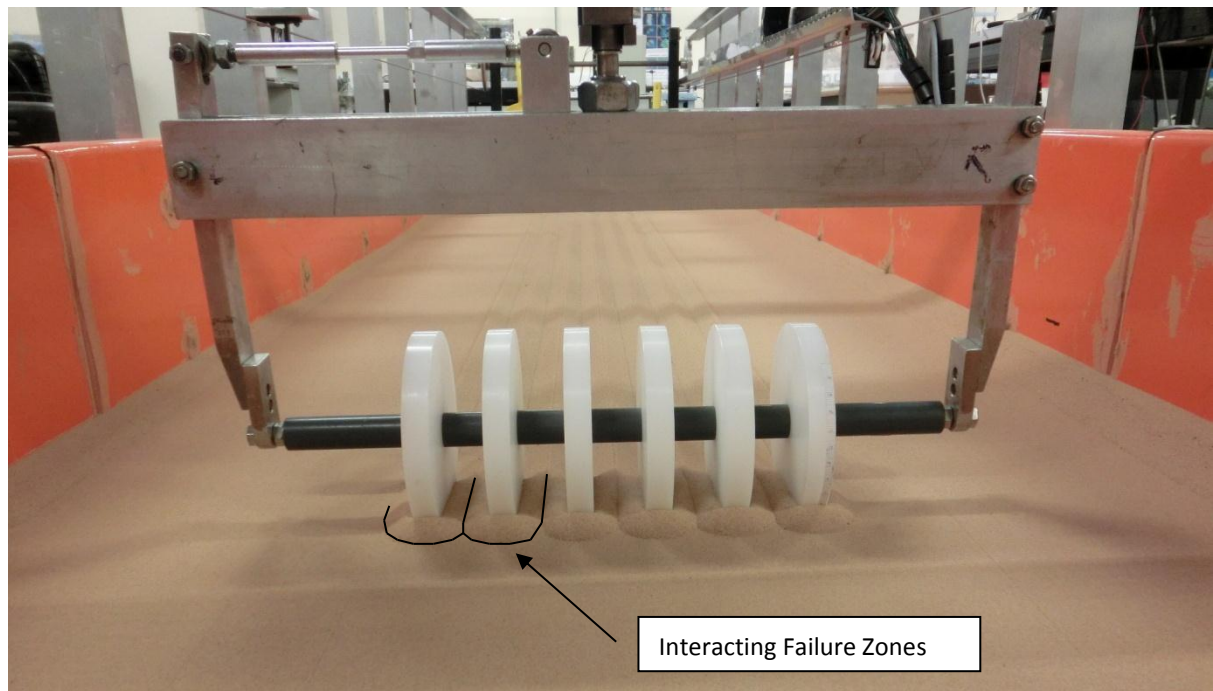
Figure 25 Disks arrangement with 30mm spacing
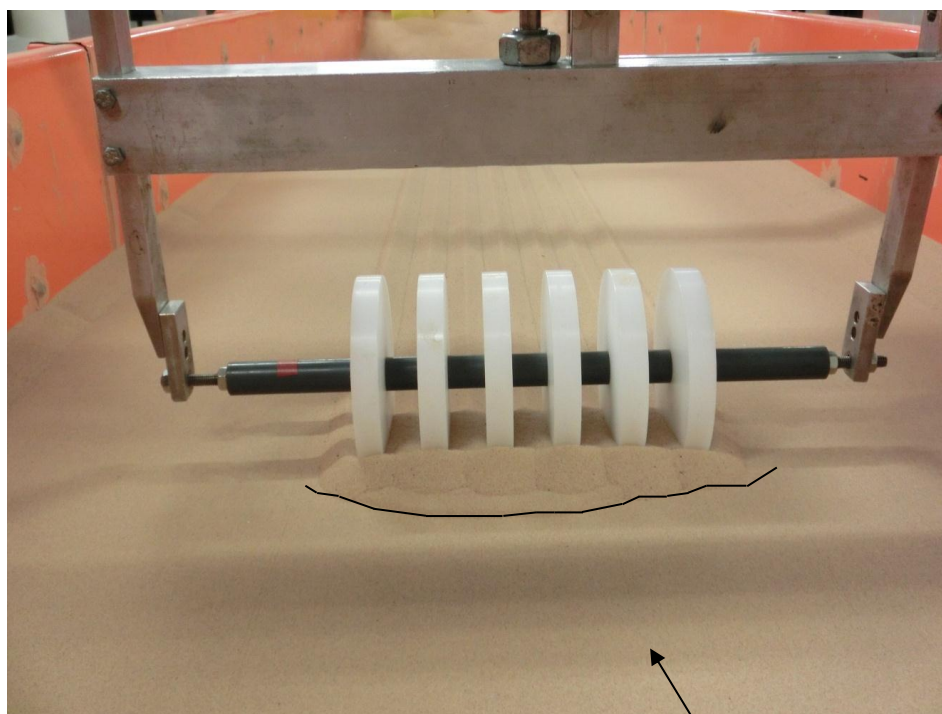
Figure 26 Disks arrangement with 22.5mm spacing

Roller-Clump

Study with roller clump is focused in the effect of the penetration depth on the ground forces. Figure 27 presents results for the drag and vertical component. Note that the upwards direction of the vertical component. Forces tend to increase linearly with the increase of the penetration depths. However, for the range of penetration depths between 1 and 5mm depth at the increase presents some curvature.
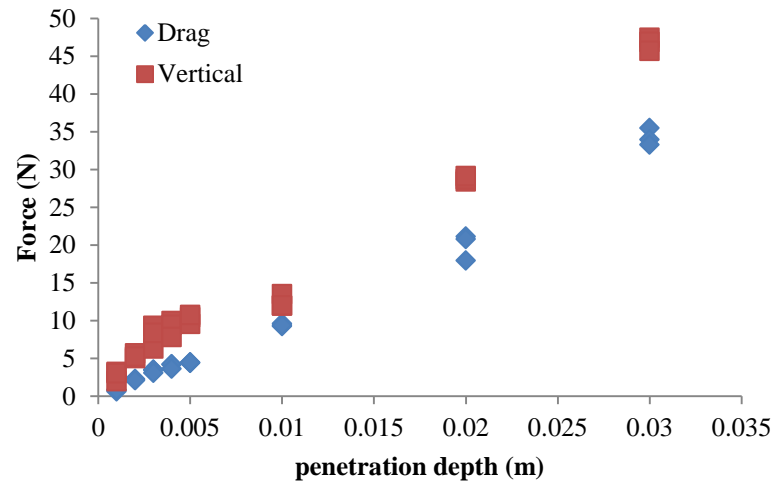
Figure 27 Ground reaction drag and vertical component evaluated with the 1:5 reduced scale roller clump when dragged at different penetration depths in dry sand at loose conditions.

Sea trials

Experimental sea trials were carried out on the RV Alba na Mara during October 2013 in the inner Moray Firth, Scotland (Figure 28).
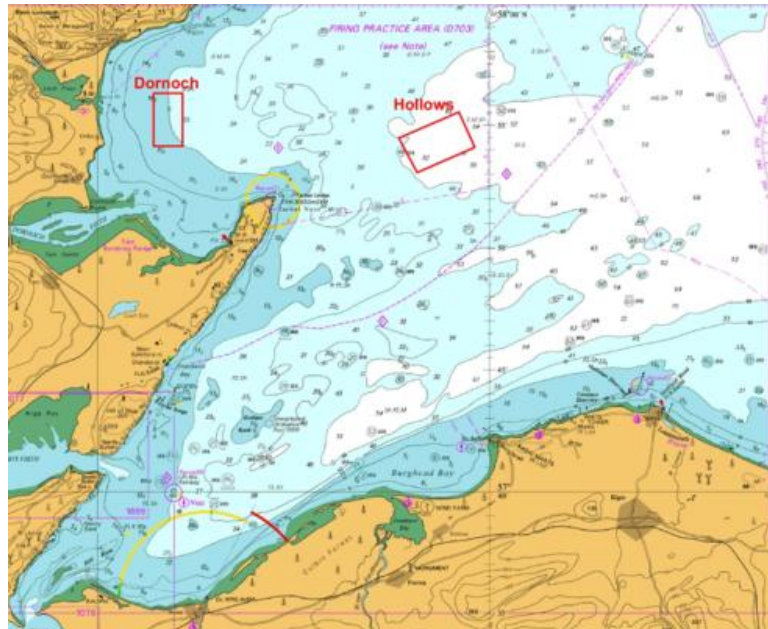
Figure 28. The inner Moray Firth where the trials took place.

A towed sledge, of height 0.9m, width 2.1m, length 3.0m and weight 530kg was used to tow a range of cylindrical and rectangular objects supported on an axle, which were chosen to simulate a range of gear elements that are in contact with the seabed (groundgear, doors, clumps etc) (Figure 29).

Figure 29. The towed sledge used to tow the range of cylindrical objects supported on an axle.

The full range tested is presented in figure 30 and includes disks and cylinders of diameter 200, 300 and 400mm, and rectangular doors of width 600mm and height 200, 300 and 400mm. In total 14 different configurations were examined, eight different cylinder designs, three configurations of separated disks and three of rectangular doors.
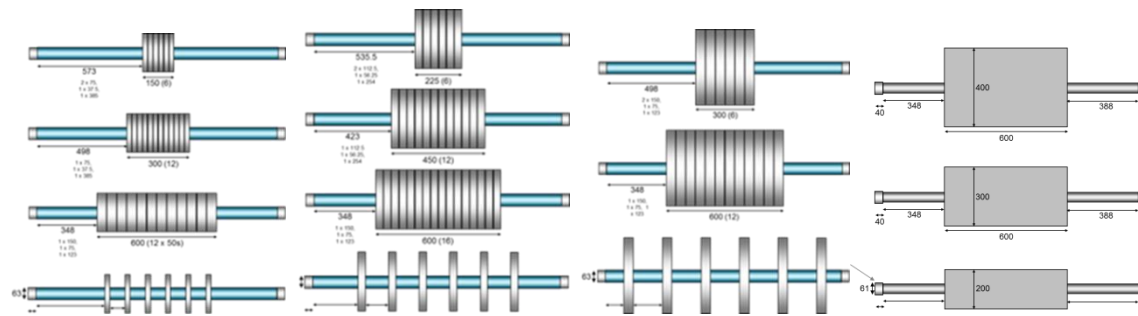
Figure 30. The range of gear components chosen to simulate some of the groundgears, clump weights and doors used in demersal fisheries comprising disks, cylinders and doors of diameter/heights 200, 300 and 400mm.

These were fixed onto an axle that is 1.3m long and of 63mm in diameter and Strainstall 500kg X-Y load cells were fitted at each end of the axle to measure forces in the horizontal plane at a rate of 10Hz. The axle was attached to a framework (via the load cells) that was free to move in the vertical direction (Figure 31).
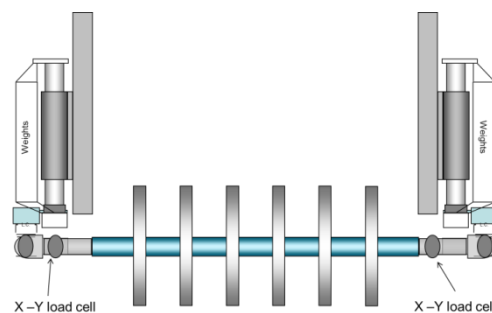
Figure31. The framework to which the gear components and axle were attached showing where the additional weights were fitted and the position of the two Strainstall 500kg X-Y load cells.

Hence, the vertical forces the gear elements exerted on the sea bed were the gravitational forces associated with the gear element and that part of the supporting framework that was free to move. It was also possible to increase the applied vertical forces by attaching weights to the framework and each of the configurations was tested having vertical weights (in water) of approximately 60, 120 and 180kg. During each deployment the speed at which the sledge was towed was increased incrementally over a thirty minute period from 1 to 2 m/s. The vessels GPS recorded the speed of the sledge over the ground at a rate of 1Hz.

Hydrodynamic drag measurements were taken when the elements were not in contact with seabed; while combined hydrodynamic and geotechnical measurements were taken when the elements were in contact with the seabed.

To classify the sediment on which the trials took place, 15 grab samples were taken with a modified Day grab and the top 2.5 cm sampled and frozen. An average was then taken to characterise the particle size distribution at the site.

Contact/geotechnical drag

To calculate the contact (geotechnical) drag, the hydrodynamic drag was subtracted from the measured drag. The experiments with the cylinders and circular disks took place both when they were permitted to roll and when they were held fixed.

In order to standardise and compare the data we consider the drag and weight per unit area where the area scale for the cylinders is *bd*, for the disks it is 6*bd* and for the doors it is *bt* where *t* is the door thickness. Initial analysis of the data suggests that the geotechnical drag per unit area has a linear dependence on the towing speed and a quadratic one on weight per unit area. Furthermore, Hambleton

and Drescher (2009) have shown that for cylinders on cohesive sediments there is a dependency on the diameter to breadth ratio (*d/b*) and whether cylinders are rolling or fixed. Hence, the data were categorised accordingly, and fitted to curves of the form

$$D = \alpha_1 W + \alpha_2 UW + \alpha_3 W^2 + \alpha_4 UW^2$$

for a given *d/b* value and a rolling or fixed state. The data from the three door designs were also fitted to a similar type of curve.

Results and Conclusions.

The geotechnical drag measurements for the gear elements are presented in figures 32 and 33. The three data sets (coloured light grey, grey and black) in each individual plot relate to the vertical forces of 60, 120 and 180kg. These figures plot the drag per unit area data against towing speed for the eight cylinders and the three sets of circular disks when they are held fixed and when they are permitted to roll respectively. The black lines are the corresponding model predictions of this relationship between evaluated at each of the three applied vertical forces and the appropriate *d/b* category for each component. These plots demonstrate

(i) that the geotechnical drag increases as the weight of the component increases;

(ii) that, for the rolling circular disks and cylinders, the geotechnical drag tends to increase as the speed increases, and

(iii) that, for the fixed circular disks and cylinders and the trawl doors, the geotechnical drag tends to decrease as the speed increases.

Figures 34 and 35 plot the same data, but this time in terms of weight per unit area, for each *d/b* category. The lines on each plot are the model predictions of the drag per unit area versus weight per unit area at a towing speed $U = 1.54$ ms^{-1} (the average value across the trials).

Figure 36 plots all the fitted curves of figures 34 and 35 and demonstrates that

(i) the drag of the fixed elements is greater than that of the rolling ones;

(ii) that the drag of the fixed cylinders is greater than the drag of the fixed disks; and that

(iii) the drag of the rolling cylinders and disks are very similar.
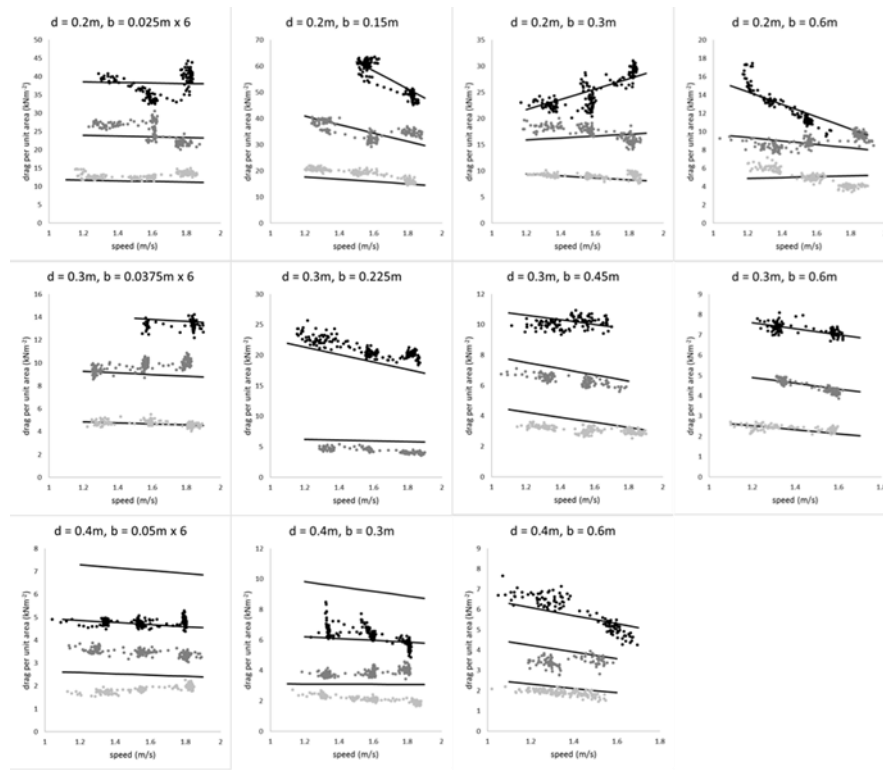
Figure 32 The geotechnical drag measurements for the fixed circular disks and cylindrical components plotted against towing speed.
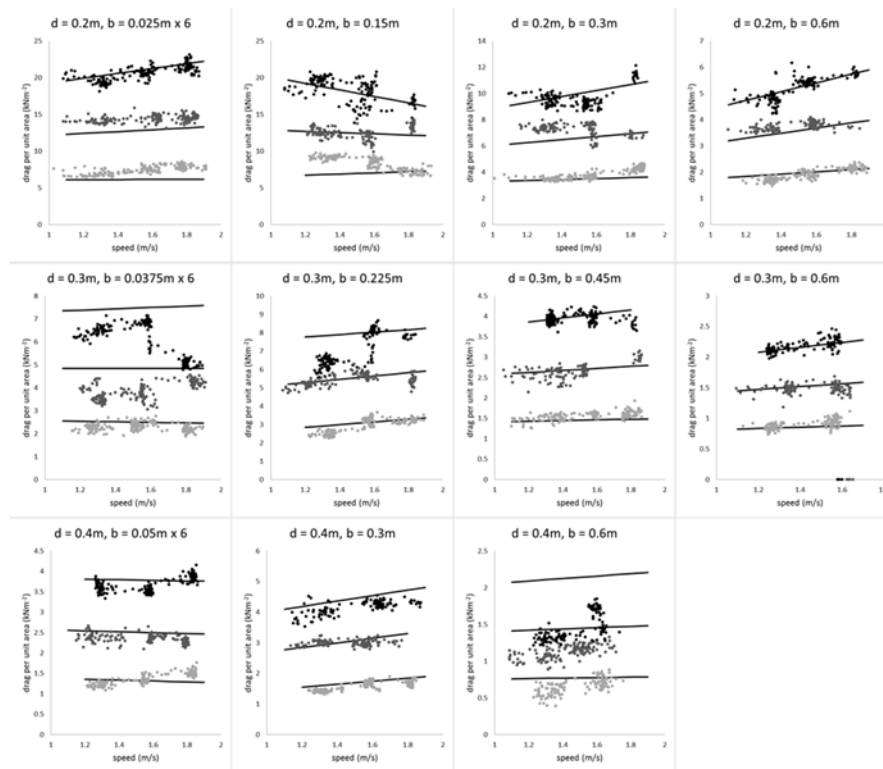
Figure 33 The geotechnical drag measurements for the rolling circular disks and cylindrical components plotted against towing speed.
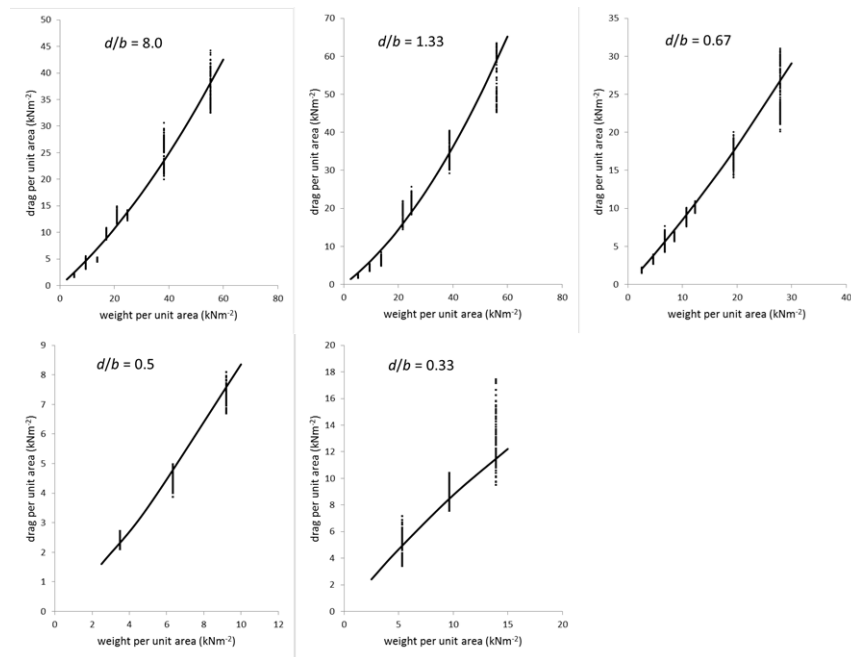
Figure 34 The geotechnical drag measurements for the fixed circular disks and cylindrical components plotted against weight per unit area.
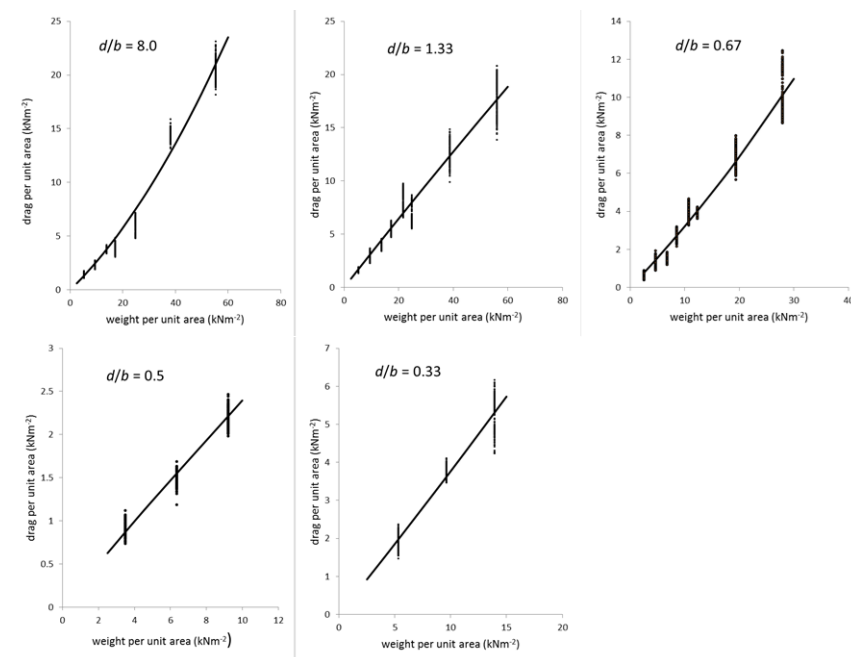
Figure 35 The geotechnical drag measurements for the rolling circular disks and cylindrical components plotted against weight per unit area.
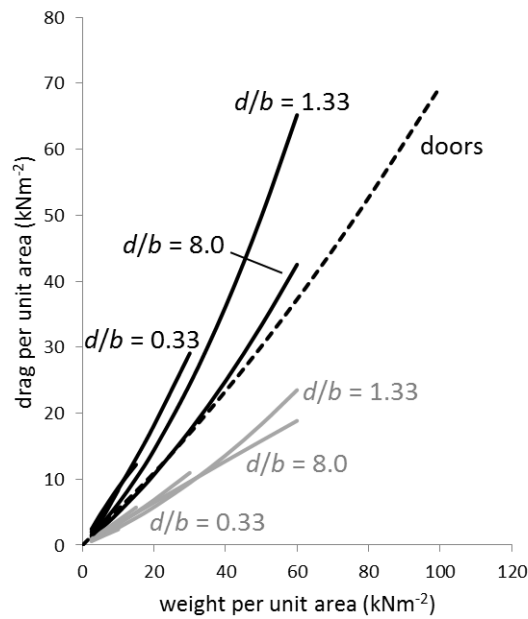
Figure 36 The fitted curves of figures 34 and 35. The black lines are for the fixed cylinders and disks and the grey lines are for the rolling cylinders and disks.

5 MODEL VALIDATION

Sandy sediment

As part of sea trials a number of different experiments were undertaken as part of sea trials performed by Marine Scotland Science in 2014.

In order to refine the model a range of densities (2000 – 2500kg/m^3) and Young Modulus (10 – 50 MPa) were selected which required a number of simulations to be run. The final material properties used in these simulations are as shown in Table 6. This model was more accurate than that used previously and the simulations undertaken on a range of roller clump models (see Table 7) show a very good match between the numerical and experimental results. (Figure 37)

Table 6 Material properties

Specific weight γ (kN/m^3)	Young's modulus E (MPa)	Poisson's ratio υ (-)	material Cohesion c (kPa)	angle of friction β (∘)	cap eccentricity	initial yield surface position	transaction surface rad	flow stress ratio
19.6	20	0.3	0.003	50	1.2	0.0	0.05	1

Table 7 Geometrical properties of the clump weight

Component	Geometry		Speed (m/s)	Weight (kg)
	Thickness (m)	Diameter (m)		
Clump	0.15 0.3 0.6	0.2	1.0 1.5 2.0	60 120 180
Clump	0.225 0.45 0.6	0.3	1.0 1.5 2.0	60 120 180
Clump	0.3 0.6	0.4	1.0 1.5 2.0	60 120 180

Since the shape of the models used in experiments is mainly of a cylindrical shape, it was used for both the clump and discs. The comparison between the results obtained as part of FE study and sea trials explained in the previous section and shown in Figure 37 show a very good comparison which validates the model for sandy sediment.
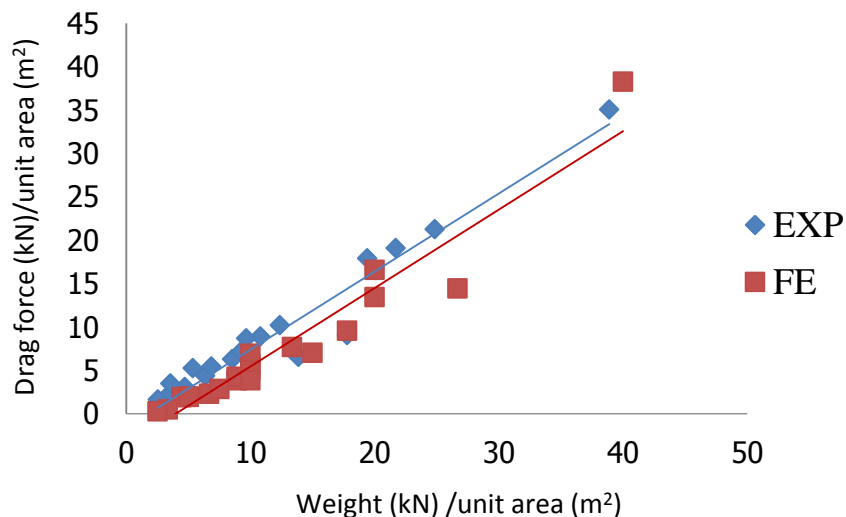
Figure 37 Comparison between the numerical and experimental (sea trials)

Muddy sediment – validation

Full-scale experiments at sea took place on board the MRV Clupea during September 2006 and October 2007 off the Moray Coast, Scotland on soft sediment type, relatively smooth soft muddy sand (off Nairn).

Figure 38. A model of a roller clump

The roller clump towed in the experiments comprises ten circular disks and a rectangular plate as shown in Figure 38. The plate has dimensions of 1.02 by 0.94m and supports a 0.1m diameter cylindrical axle, on to which the disks are mounted and around which they can rotate. The disks have outer and inner diameters of 0.58 and 0.11m respectively and are between 0.04 and 0.05m in width. The summed width of all the disks is 0.495m and the total weight of the clump assembly is 11.8kN in air and 9.7kN in water.

On muddy sand the roller produced a well defined trench of 100-150mm depth after towing. It was also observed that the disks of the roller did not roll when it was towed on this sediment and hence the FE model was run under similar conditions. See comparison of results in Figure 39.
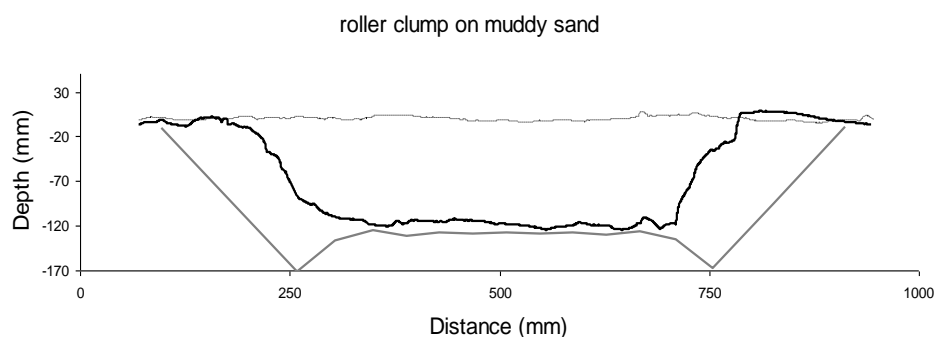
Figure 39. Comparison between the results obtained for the roller clump from FE and seatrials

The FE model predicts a build-up of the sediment in front of the roller which is then displaced to the sides producing a hardening effect. This is connected to large strains due to the towing process and indicates that the simulated drag force consists of two main components, a base friction and a passive pressure from the build-up of soil in front of the roller clump. This build-up of sediment is not so apparent in the sea trials and it is likely that material properties of the muddy sand sediment were non-homogeneous and may have a softer and potentially looser top layer which results in compaction of the sediment rather than a build up at the front and the sides.

32

6 MODEL PREDICTION

Sandy sediment

The simulations for other gear elements – otter door and ground gear elements have also been undertaken. Two cases of ground gear elements were looked into (Figure 40).
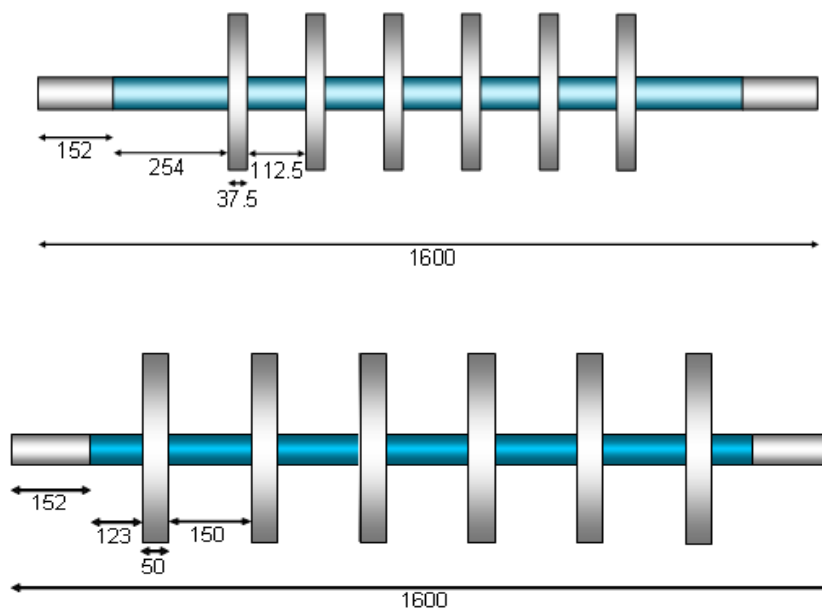
Figure 40 Schematic view of the ground gear assemblies (200mm dia of the top and 400mm dia of the bottom)

The Mohr–Coulomb failure criterion represents the linear envelope for peak stresses obtained from the shear box tests undertaken at several relative densities, (i.e. loose $D_r = 15\%$, medium dense $D_r = 48\%$ and dense $D_r = 70\%$) at normal effective stresses of 10-150 kPa when c is fixed at zero. Lauder (2011), however note that the peak angle is higher at lower normal effective stresses. This study shows that the shear and normal effective stresses relationships show a slight non linearity at normal effective stresses less than 10 kPa. For instance, the peak friction angle $\varphi_{peak} = 60°$ over the normal effective stress range 1-5 kPa for $D_r = 75\%$ decrease to $\varphi_{peak} = 44°$ for higher normal effective stresses of 10-70 kPa. Lauder (2012) indicate that the tests conducted at lower effective stresses show higher level of dilation whereas the tests conducted at the higher normal effective stresses show the least dilation. The influence of the peak friction angle on normal effective stress was therefore deemed important to the numerical modelling of the small scaled model conducted at low levels of normal stress. As this study is attempted to model the interaction between an object with the sand in loose condition, the angle of internal friction of Mohr-Coulomb constitutive model used in FE simulation is based on the critical angle of friction.

Muddy sediment

The parametric study work undertaken after the model was validated has shown a great potential to estimate penetration and drag forces depending on the properties of the gear elements and soil properties.
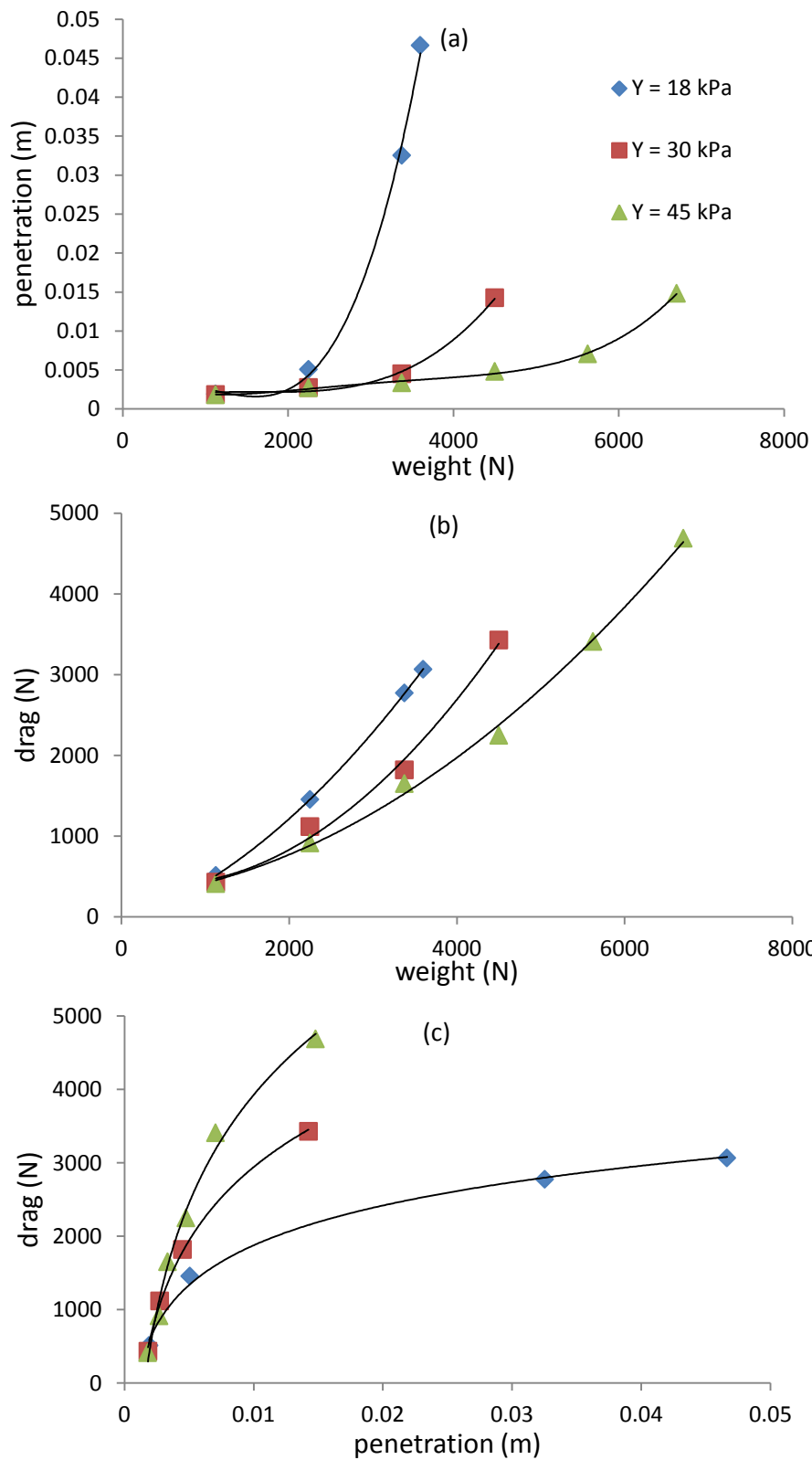
Figure 41. The averaged steady state values of (a) penetration depth vs weight, (b) drag vs weight (c) drag vs penetration for a circular clump on a soil

Figure 41 (a) and (b) demonstrate that as the yield stress increases the penetration decreases and that this leads to an associated reduction of the drag on the clump. However, as would be expected, it is also apparent that for the same penetration the drag is greater when the yield stress is larger (Fig. 41(c)). Likewise, Figure 42(a) shows how, as the soil becomes stiffer, (ie as the Young's modulus, E, increases) the penetration into the soil decreases. However, over the parameter range examined here, there does not appear to be any systematic relationship between drag and soil stiffness (Figure 42(b)). This is probably due to the fact that the penetration is small, and that consequently the main contribution to drag is from the bottom surface contact. In the same way as for the yield stress (in Figure 41(c)), it is also clear that for the same penetration the drag is greater on the stiffer soil (Fig. 42(c)).
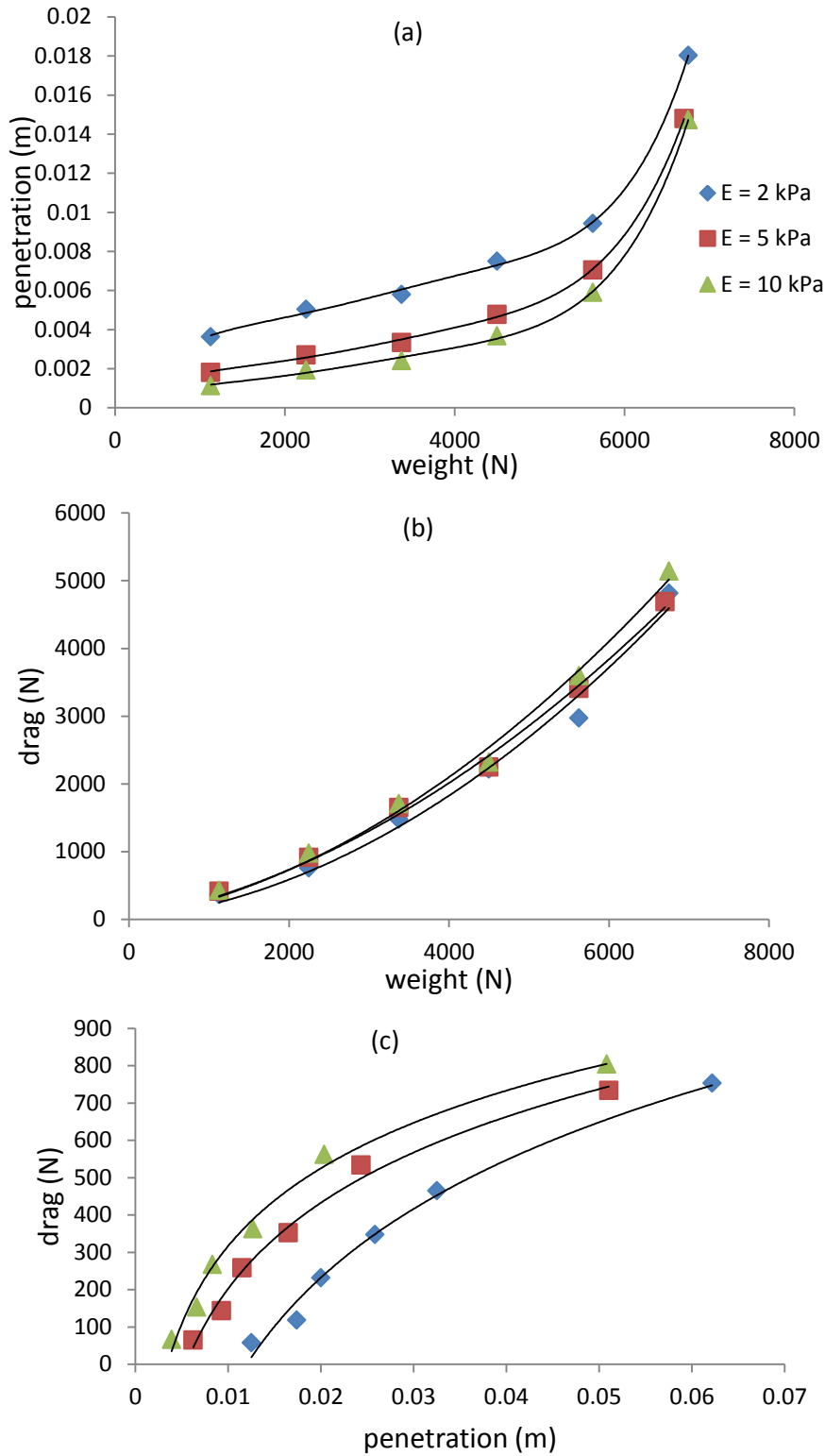
Figure 42 (a) penetration depth vs weight; (b) drag vs weight (c) drag vs penetration

7 MODEL CAPABILITIES

The influence that the dimensions, the weight, the cross-sectional geometry and the soil material properties have on penetration and drag of truncated rigid cylinders towed on fully saturated muddy soils and sandy soils have been investigated.

In general, over the parameter ranges examined for the muddy sediment:

- there is a non-linear increase in penetration and drag as the weight increases;
- there is a decrease in penetration and an associated reduction of drag as the Yield stress and Young's modulus increase.
- We also examine the non-dimensional form of the problem and demonstrate that the penetration and drag values reduce respectively to single curves that are dependent solely, at least to a first order of approximation, on the non-dimensional weight, suggesting that the problem is essentially two-dimensional in nature and that three-dimensional effects at the edges of the clumps do not play a significant role.

Similar results were presented by Hambleton and Drescher (2008) who found that, for rigid cylinders on clays, there was no dependence on aspect ratio. On sands, however, and for rolling cylinders on drained soil, aspect ratio and three-dimensional effects have been shown to be significant (Hambleton and Drescher, 2009. These contrasting results highlight the need to ensure that our results are used appropriately. The elastic-perfectly plastic model, which we have used with a Poisson's ratio of 0.5, over a Young's modulus range of 2 – 10 MPa, relates to fully saturated soft clayey soils. Hence the formulations should apply to these types of substrates. In a fisheries context these include the highly productive muddy soils which support many important commercially exploited species such as Nephrops norvegicus (langoustine) and many species of demersal fish.

The results obtained for the two types of ground gear towed along the sandy sediment are shown in Table 8.

Table 8 Comparison results FE and sea trials for two types of ground gear (see gear details in Figure 40)

Component	Finite Element Method			Experiment	
	Mass (kg)	Drag force (N)	Penetration (m)	Mass (kg)	Drag force (N)
Case 1	588	210	0.022	644	324
Case 1	1176	537	0.050	1160	652
Case 1	1764	1018	0.070	1676	896
Case 2	588	150	0.012	632	217
Case 2	1176	398	0.029	1148	419
Case 2	1764	697	0.048	1664	570

As can be seen the smaller diameter of the ground gear (Case 1) produces larger penetration that that of Case 2 which indicates that they act as a cutting tool. A good comparison between the experiment and finite element results are shown in Figure 37.
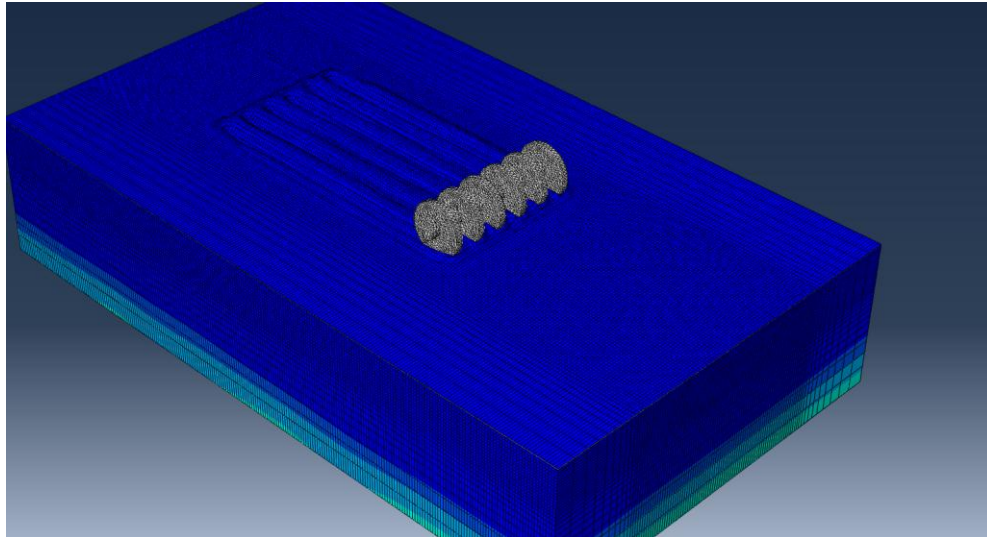
Figure 43 An image from Abaqus (rockhoppers on sandy sediment)

Simulations on otter door provided the following results (Table 9) indicating clearly that the otter door produce more penetration than the rock hoppers.

Table 9 Comparison results FE and sea trials for the otter-door

Length (m)		Width (m)	Depth (m)	Angle of attack (○)	Mass(kg)	Drag force (N)	Penetration (m)
1.83		0.169	0.16	35	300	2320	0.037
1.83		0.169	0.16	35	380	2698	0.044
1.83		0.169	0.16	35	460	3913	0.075
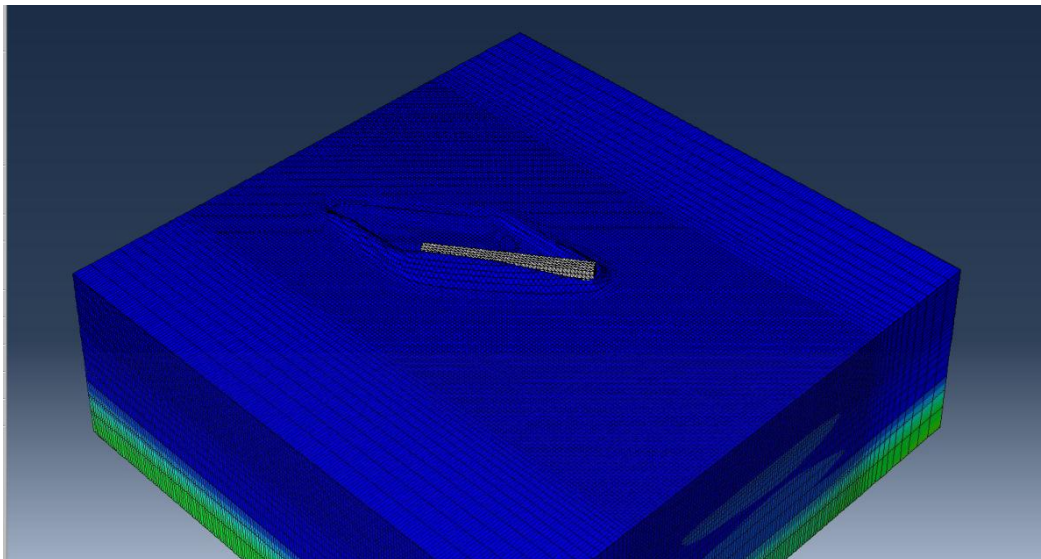
Figure 44 An image from Abaqus (otter door shoe on sandy sediment)

Connection with other work packages

The model was successfully used as part of the case study at the North Sea, details of the gear employed for the investigation is shown in Figure 45   (Depestele et al, 2015).
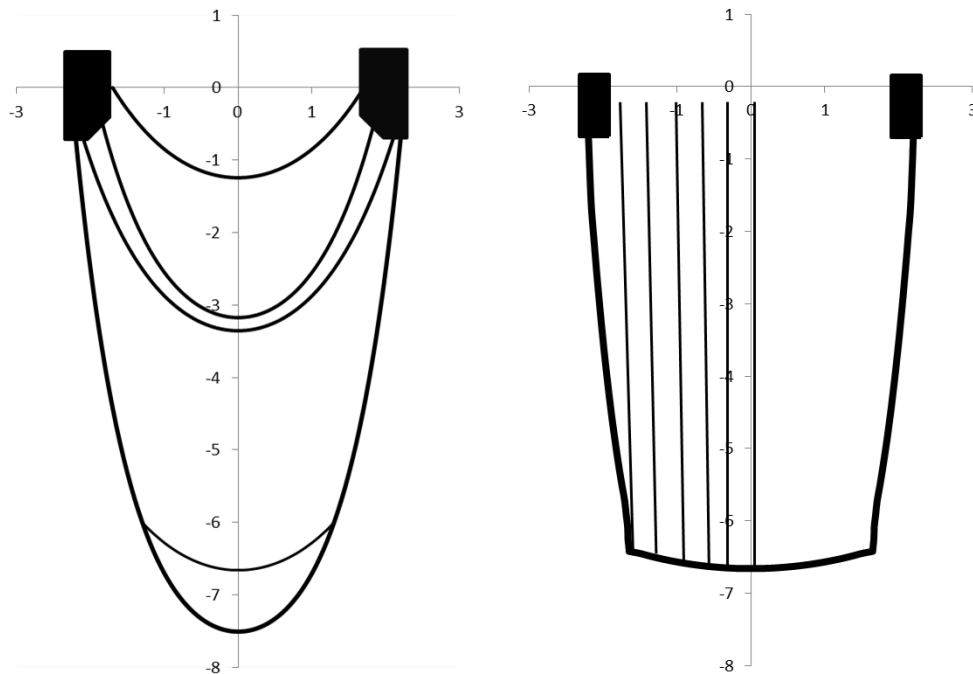
Figure 45 Gear components in contact with the seabed for the tickler chain (left) and pulse (right) trawl. Tickler chains with a chain link diameter of 28mm are attached to the trawl shoes, whereas the tickler chains of 11 to 16mm are attached to the ground gear (only one is shown). [Depestele et al, 2015]

It has been shown that there is a very good agreement between the experimental measurements and the numerical predictions. The average penetration depth across the full swept area of the gear was predicted to be 9 mm which compares very well with the MBES measurements.

The model in general gives a good indication of its potential and the current developments regarding the inclusion of the water in the laboratory sand channel will allow even better estimation of the real physical processes. The current model is somehow restricted to the software used.

8   CONCLUSIONS

The report reviews the work that has been undertaken in relation to the observation, quantification and estimation of the immediate physical impacts of trawl gears on soft sediments. It is based on reduced scale laboratory modelling, full scale sea trials and FE numerical modelling, leading to the identification and understanding of the physical processes happening within the seabed sediment during the passage of trawl gears. Such an understanding is key predicting the areas of potential disturbance and therefore the affected volume of sediment. This is directly related to the disturbance of benthic ecosystems and the ground resistance (geotechnical drag) acting opposite to the towing direction. The capability to predict

the seabed disturbance is a function of the gear characteristics (geometry, weight, material and/or distribution on the fishing line) will lead to the development of more environmentally friendly fishing gear.

Evidence of the potential processes happening within sandy sediment during trawling were observed experimentally. These processes are related to the sediment failure mechanisms associated to passive earth pressure acting at the contact area between the gear and the seabed. From this, analytical prediction of the volume of the sediment affected by the gear was proposed as a function of the sediment and gear characteristics as well as their penetration into the ground. As expected, greater sediment disturbance was found for the deeper penetration evaluated (see Figure 19 and Figure 27). Since one of the main functions of the ground gear is to ensure ground contact, a balance has to be found between the penetration of the gear into the ground (mainly a function of the gear geometry and weight) and its functionality, by including lighter gear or altering the geometry. One possibility is to use an aerofoil shape. An aerofoil shaped gear has a smaller hydrodynamic drag and penetrates the seabed less (Ivanović & O'Neill, 2015). Another way to optimise the ground contact comes from the alteration of the space between the elements/discs of the ground gear. Experimentally it was found an increase of the affected volume of sediment, noticed by the increase of the geotechnical drag with the decrease of the separation between disks in an assembly of six disks (Figure 22) due to the interaction of sediment failure zones resulting in a general failure involving all six elements at once. To avoid sediment failure interaction between narrow disks a separation (s) of s/z>2.86 is suggested, where z is the penetration depth. Regarding the effect of the position of the gear fishing line defined by the inclination with the respect to the towing direction (acting at an angle of attack), no effect on the forces (and therefore the affected volume of sediment) is found (see Figure 21 and Figure 22).

Full scale sea trials provided a set of geotechnical drag measurements for a wide range of gear geometries and weights (see Figure30). Those tests were undertaken along both sandy and muddy seabed. A greater geotechnical drag is found for the heavier elements, since greater penetration depths are expected and therefore greater sediment was displaced. While the reduced scale modelling cylindrical models in the laboratory experiments were not allowed to roll, in sea trials both rolling and not rolling cases were evaluated. Two different trends were found for the fixed and not rolling case with the increase of the velocity. For the rolling circular disks and cylinders, the geotechnical drag tends to increase with the increase of the towing velocity. On the other hand for the fixed disks and cylinders, the geotechnical drag tends to decrease with the increase of the velocity. However, by keeping the velocity constant, lower geotechnical drag is measured for rolling and lighter models, since less penetration into the ground is achieved. Therefore, the fishing line has to be composed by the minimum possible number of elements, and where possible, allowing them to roll and keeping the system as light as possible, but ensuring functionality and the robustness of the system. On muddy seabed, rolling of the gear is not possible due

to the adhesive properties of the ground. In this case, aerofoil shaped gear can be placed along the fishing line in order to keep the ground contact at minimum.

The numerical model developed allows the evaluation of the penetration depth and effect on the seabed to be defined as a function of the gear geometry and dimensions, weight and the seabed properties for sandy and muddy sediments. The model was validated from both the reduced scale experiments and sea trials and very good agreement was found. From numerical simulations on muddy seabed, a non-linear increase in penetration and drag as the weight of the gear increases. By examining the non-dimensional form of this problem it was found that the penetration was dependant solely on the non-dimensional weight, suggesting that the interaction of ground gear with muddy seabed is two-dimensional with no effect related to the aspect ratio of the cylindrical element. This analysis led to the expression for the prediction of the penetration into the seabed as a function of the weight, geometry of the gear and yield stress (Ivanović & O'Neill, 2015).

RECOMMENDATIONS

Proposed measures to develop gears that are more environmentally friendly:

1. Lighter gears, ensuring functionality.
2. Introduce aerofoil shapes.
3. Optimise the distance between the elements/disks in the ground gear (for narrow disks s/z>2.86).
4. Keep the ground gear rolling, where possible.
5. Ground gear distribution:
   a. If not rolling, lower drag per unit length for narrower cylinders (and disks) is found. Optimisation of the ground gear by using narrower and lighter cylinders and reducing the number of them.
   b. If rolling, there is no effect of the width on the drag force per unit length. Optimisation of the width and distribution by keeping the contact area with the ground to a minimum.
6. Make use of the current models to evaluate the penetration of the gear into the ground.
7. Despite that in some cases, a reduction of the disturbed sediment may be achieved by increasing the width of the gear, an evaluation from an ecological point of view will determine if a smaller area of more deeply impacted seabed is preferable than a larger area of a less deeply impacted.

REFERENCES

Arntz W. & W. Weber (1970) Cyprina islandica (Mollusca: Bivalvia) als Nahrung von Dorsch und Kliesche in der Kieler Bucht. Berichte der Deutschen Wissenschaftlichen Kommission für Meeresforschung 21, 193-209.

Bessonneau J.S., Marichal D. Study of the dynamics of submerged supple nets, Ocean Engineering, 27, (7), 1998, 563-583.

Bridger, J.P., 1970. Some effects of the passage of a trawl over the seabed. ICES C.M. 1970/B:10.

Caddy, J.F., 1973. Underwater observations on tracks of dredges and trawls and some effects of dredging on a scallop ground. Journal of the Fisheries Research Board of Canada 30, 173-180.

Clark, R.A., Frid, C.L.J. 2001. Long-term changes in the North Sea ecosystem. Environmental Reviews 9, 131-187

Dounas, C., Davies, I., Triantafyllou, G., Koulouri, P., Petihakis, G., Arvanitidis, C., Sourlatzis, G., and Eleftheriou, A., 2007. Large-scale impacts of bottom trawling on shelf primary productivity. Continental Shelf Research. 27: 2198 – 2210.

Esmaeili M and Ivanović A, 2015, Analytical and numerical modelling of the interaction of rigid element with friction material' Computers and Geotechnics, Volume 68, 208–219.

Esmaeili M. and Ivanović A., 2014 Numerical Modeling of Fishing Ground Gear Component on the Seabed, Ocean Engineering, 91, 316–328.

Gilkinson K., Paulin M., Hurley S., Schwinghamer P., 1998. Impacts of trawl door scouring on infaunal bivalves: results of a physical trawl door model/dense sand interaction, Journal of Experimental Marine Biology and Ecology, 224, 291-312.

Hambleton J.P. and Drescher A, 2008. Modelling wheel-induced rutting in soils: Indentation, Journal of Terramechanics, 45, 201-211.

Hambleton J.P. and Drescher A, 2009 (a) Modelling wheel-induced rutting in soils: Rolling, Journal of Terramechanics, 2009(a); 46: 35-47.

Hambleton JP and Drescher A, On Modelling a roller wheel in the presence of plastic deformation as a three – or two- dimensional process. International Journal of Mechanical Sciences 2009 (b); 51: 846-855.

Igland R.T. and Søreide T., 2008. Advanced pipeline trawl gear impact design. Proceedings of the ASME 27th International conference on Offshore Mechanics and Arctic Engineering, OMAE 2008, June 15-20, Estoril, Portugal.

Ivanović, A. and O'Neill F.G., 2015, Towing cylindrical fishing gear components on cohesive soils. Computers and Geotechnics, 65, 212-219.

Ivanović, A., Neilson, R.D., O'Neill F.G. 2011, Modelling the physical impact of trawl components on the seabed. Ocean Engineering.; 38(7): 925-933.

Jones, J.B., 1992. Environmental impact of trawling on the sea-bed: a review. New Zealand Journal of Marine and Freshwater Research 26, 59-67.

Kaiser, M.J., Collie, J.S., Hall, S.J., Jennings, S. and Poiner, I.R., 2002. Modifications of marine habitats by trawling activities: prognosis and solutions. Fish and Fisheries, 3, 114 – 136.

Khandriche, A., Werner, F., Erlenkeuser, H., 1986. Auswirkungen der Oststürme vom Winter 1978/1979 auf die Sedimentation im Schlickbereich der Eckernförder Bucht (westlichr Ostee). Meyniana 38, 125-152.

Krost, P., Bernhard, M., Werner, F., Hukriede, W., 1990. Otter trawl tracks in Kiel Bay (Western Baltic) mapped by side-scan sonar. Meeresforschung 32, 344- 354.

Le Dret, H., Priour, D., Lewandowski, R., and Chagneau, F. (2004). "Numerical Simulation of a Cod End Net Part 1: Equilibrium in a Uniform Flow." Journal of Elasticity, 76(2), 139-162.

Lindeboom H.J., Groot, S.J. de (editors), 1998. The effects of different types of fisheries on the North Sea and Irish Sea benthic ecosystems. IMPACT-II Report. Chapters 2. Materials and Methods, and 3. Results; Ottertrawls - Immediate effects pp. 19, 126-127.

Løkkeborg, S., 2005. Impacts of trawling and scallop dredging on benthic habitats and communities. FAO Technical Paper No. T472. Food and Agriculture Organization of the United Nations, Rome.

Nouguier, C.,Bohatier C. Morean J.J., Radjai F., 2000. Force fluctuations in a pushed granular material. Granular Matter, 2, 171–178

O'Neill F.G, 1997. Differential equations governing the geometry of a diamond mesh cod-end of a trawl net, Journal of applied mechanics, March 1997, Vol. 64/7, 453, p. 1631-1648.

O'Neill F.G., 1999. Axisymmetrical trawl cod-ends made from netting of generalized mesh shape. IMA Journal of Applied Mathematics 62, 245-262.

O'Neill, F.G., Neilson R. D., 2008. A dynamic model of the deformation of a diamond mesh cod-end of a trawl net. Journal of Applied Mechanics, 75, 1, [DOI: 10.1115/1.2755153],.

Palmer A.C. Speed effects in cutting and ploughing. Geotechnique 1999; 49: 285-294.

Paschen, M. et al, 2000. TRAPESE Final Report on DG XIV – Fisheries Contract No 98-006.

Prat J., Antonijuan J., Folch A., Sala A., Lucchetti A., Sardà F., Manuel A. 2008 A simplified model of the interaction of the trawl warps, the otterboards and netting drag, Fisheries Research, 94, (1), 109-117.

Priour, D.,1999. Calculation of net shapes by the finite element method with triangular elements. Communications in Numerical Methods in Engineering, 15(10), 755-763.

Rességguier S., Bendzovski R.,Strøm P.J, Wathne H., Vigsnes M., Holme J.,2009. Assessment of trawlboard and anchor penetration in different soils for use in selection of a burial depth to protect submarine cables or pipelines. Proceedings of the ASME 28th International Conference on Ocean, Offshore and Arctic Engineering, OMAE 2009.May31-June 5,Honolulu, Hawaii.

Zhao, Y., Miedema, S.A. 2001. Finite element calculations to determine the pore pressures when cutting water saturated sand at large cutting angles. [C]//CEDA Dredging Days,